Università di Camerino

Ph.D. Thesis

Transmission of Classical Information through Gaussian Quantum Memory Channels

Oleg Pilyavets

Supervisor

Dr. Stefano Mancini

Camerino, 2010

Contents

Abbreviations

Below abbreviations used in the text of thesis are given.

BS — beam-splitter
HUR — Heisenberg uncertainty relation
LBC — lossy bosonic channel
LBMC — lossy bosonic memory channel

Introduction

Quantum communication is a relatively new area which is a part of *quantum information theory* devoted to study information transmission through *quantum channels*. By quantum channels are intended all means that convey quantum systems on whose states information is encoded. Formally they are *quantum maps* from input to output states [1]. The study of quantum channels is necessary not only for quantum communications purposes, but also for *quantum computing* and *quantum cryptography*. Quantum channels can be used to transmit *classical information* besides *quantum information*. In fact, classical symbols can be encoded/decoded into/from quantum states sent through quantum channels.

The main objective of quantum communication is the characterization of the transmission capabilities of quantum channels. The maximum rate at which information can be reliably transmitted through a quantum channel defines its *capacity*. Actually, one can define several capacities depending on the kind of information transmitted (classical or quantum) and on the additional resources used in transmission [2]. Evaluation of quantum channels capacities is one of the most important and difficult problems in quantum information theory.

A *memoryless* quantum communication channel makes the fundamental assumption that the noise in consecutive uses of the channel is independent. This assumption is reasonable for many real-world applications, but for many others the noise may be strongly correlated among different channel uses. Recently a lot of efforts have been dedicated to the development of quantum models that encompass memory effects (see [3] for an overview). One of the main motivations that has led to investigate such effects in quantum channels has been the possibility to enhance their classical capacity by means of entangled inputs. Such a possibility has been recently put forward in *channels with continuous alphabet* [4-7]. However, most of these works were limited to provide a proof of principle of the behavior of quantum memory channels. Since the notion of capacity is intimately related with the asymptotic behavior of a channel, there is a persistent wish to move on from small to large (towards infinite) number of channel uses. Channels with continuous alphabet are realized in the quantum framework by boson algebra (each input, respectively, output is represented by a bosonic field mode). Among them, *Gaussian channels*, which maps input Gaussian states into output Gaussian states, are the simplest allowing capacities investigation [8, 9] and are also easy to implement experimentally [10]. The *lossy bosonic channel* (LBC), which consists of a collection of bosonic field modes that lose energy en route from the transmitter to the receiver [10] belongs to the class of Gaussian channels. The effect of losses is usually modelled by letting each input mode to interact with an environment mode through a rotation (beam-splitter) transform whose angle (transmissivity) determines the loss rate [10].

The classical capacity (including that *assisted by entanglement*) for LBC was evaluated in Refs. [11, 12] by assuming each environment mode in the vacuum state. In such a case Gaussian (coherent separable) states turn out to be the optimal inputs. Then it has been proved that Gaussian inputs also suffice to determine the *quantum capacity* [13]. When more general states of environment are taken into account, even non factorized ones which give rise to memory effect [4], the evaluation of capacities becomes much more demanding.

To deal with this capacity problem, in this thesis a perturbative approach is developed by expanding the von Neumann entropy of Gaussian quantum state as a function of the symplectic eigenvalues of its quadratures covariance matrix (see [9] and [A5][1]). The method turns out to be very useful for characterizing any Gaussian quantum channels, but in this thesis it is applied only to the classical use of lossy bosonic memory channel (LBMC). Its application to *additive noise* memory channel is in progress [A6]. Exact solution which does not use this approximation is also presented in thesis.

Apart from capacities investigation, *achievable transmission rates* can be calculated assuming fixed type of information encoding and decoding. In this thesis classical capacity[2] [A5] and rates achievable by conventional decoding procedures [A1] (*heterodyne* — joint field quadrature measurements, and *homodyne* — one quadrature measurements) are studied analytically for LBMC when the problem becomes spectral for quantum states covariance matrices. The obtained results generalize those of Refs. [8, 12] for the classical capacity. In particular, new properties are discovered for this type of LBMC, such as the existence of *critical transmissivity*, and both *quadratures* and *mode symmetry violation*, which are intimately related each other and can lead to enhancement as well as decrement of information transmission. This poses the question of optimal memory model if average amount of photons per mode allowed in environment is fixed.

If problem is spectral for quantum states covariance matrices, the type of memory model is unitarily equivalent to another model with all matrices being diagonal, which has the same capacity but is simpler to investigate. The environment of that model is a multimode squeezed state which has no correlations among channel uses. This procedure of reducing a memory channel problem to a memoryless one has been termed *memory unravelling* [A4]. In this way the study of memory effects is traced back to the investigation of the role played by a single mode squeezed environment. In fact all interesting features of memory arising from a multimode squeezing environment can be found in single mode squeezed environment as well. The only exception is the mode symmetry violation which cannot exist for one-mode memoryless channel. Since in the memory setting the multimode squeezed states are entangled, this method allows in principle to shed light on the usefulness of correlated (classically or quantumly) input states. However, the question of how to compare different situations naturally arises.

Taking into account that the increase of squeezing always leads to increase of average amount of photons, this thesis fixes the last parameter for the set of models to compare. Then, it is shown that squeezed environment can increase or decrease the capacity depending on values of its squeezing and beam-splitter transmissivity. It is also proved that

[1] In this work the references to author's publications are prefixed with symbol A. All references are listed in chronological order.

[2] Actually, lower bound on one-shot classical capacity is calculated, as maximization is only performed over set of all admissable Gaussian states. The maximization over small subset of Gaussian states made in [A1] before the work [A5] was published has now only hystorical interest.

squeezing of environment leads to optimal inputs to be also squeezed if the restriction on average amount of input photons is not very low. Moreover, if this amount is sufficiently high the optimal input squeezing equals that of environment, *i.e.* optimal input state is correlated in the multimode setting.

Most of the results are drawn by using a particular LBMC model with non-Markovian memory (below it is often refered to as Ω-*model*), which allows to characterize the asymptotic behavior of the channel for classical information transmission. The memory effects in this model are realized by considering noise correlations among environments acting on different channel uses [4]. These correlations are introduced by contiguous modes interactions which result in an exponential decay of the correlations over channel uses (modes).

The thesis is organized as follows. In Chapter 1 basics of quantum information theory with continuous variables are discussed. In Chapter 2 LBMCs are considered and the relations for homodyne and heterodyne rates are derived as functions of involved covariance matrices. In Chapter 3 a method to find classical capacity and rates is presented for both arbitrary one-mode (memoryless) and multimode (memory) types of channels. In Chapter 4 the method is applied to a particular channel memory model (Ω-model), and some questions on optimal memory model are considered. In the Conclusions and outlook it is summarized the work done and open questions are discussed.

Publications

This thesis is mainly based on the following papers:

[A1] O. V. Pilyavets, V. G. Zborovskii, and S. Mancini: "A Lossy Bosonic Quantum Channel with Non-Markovian Memory", Los Alamos arXiv:0802.3397 (2008); *Phys. Rev.* A **77**:5, 052324-1–052324-8 (2008).

[A2] O. V. Pilyavets, V. G. Zborovskii, and S. Mancini: "A Lossy Bosonic Quantum Channel with Non-Markovian Memory", in: H. Imai (ed.), *Proceedings of 8th Asian Conference on Quantum Information Science* (Seoul, Korea, 25–31 August 2008), Korea Institute for Advanced Study, Seoul (2008), pp. 93–94.

[A3] O. V. Pilyavets, V. G. Zborovskii, and S. Mancini: "A Lossy Bosonic Quantum Channel with Non-Markovian Memory", in: A. Lvovsky (ed.), *Proceedings of 9th International Conference on Quantum Communication, Measurement and Computing (QCMC)* (Calgary, Canada, 19–24 August 2008), *AIP Conf. Proc.* **1110**:1, 123–126 (2009).

[A4] C. Lupo, O. V. Pilyavets, and S. Mancini: "Capacities of Lossy Bosonic Channel with Correlated Noise", Los Alamos arXiv:0901.4969 (2009); *New J. Phys.* **11**:6, 063023-1–063023-18 (2009).

[A5] O. V. Pilyavets, C. Lupo, and S. Mancini: "Methods for Estimating Capacities of Gaussian Quantum Channels", Los Alamos arXiv:0907.1532 (2009); submitted to *IEEE Trans. Inf. Theory*.
New comment: published with the title "Methods for Estimating Capacities and Rates of Gaussian Quantum Channels" in *IEEE Trans. Inf. Theory* **58**:9, 6126-6164 (2012).

Works in preparation:

[A6] E. Karpov, J. Schäfer, O. V. Pilyavets, and N. Cerf: "Classical Capacity of Noisy Quantum Channel with Memory."
New comment: published in J. Schäfer, E. Karpov, and N. J. Cerf, *Phys. Rev.* A **84**, 032318 (2011), where I am listed in acknowledgments.

[A7] O. V. Pilyavets, and S. Mancini: "Achievable Rates for Classical Information Transmission in Lossy Bosonic Memory Channels."
New comment: it was included as a part of the IEEE publication in [A5].

Chapter 1

Basics of quantum information with continuous variables

In this chapter basics of quantum and classical information theory together with quantum mechanics are discussed. This is to provide some standard definitions which are used in subsequent chapters. As far as this work concerns only continuous variables systems, the discrete systems (finite dimensional Hilbert spaces) are not introduced at all.

1.1 Classical probabilities and Shannon differential entropy

Standrad probability theory operates with *random variables* which can accept only discret values. Formal mathematical introduction into probability theory in the case of continuous variables is called *stochastic process theory* which becomes much more difficult and was formalized as new branch of mathematics only in the middle of previous century by A. N. Kolmogorov. However, in this introduction it is assumed that all random variables have their *probability densities*, that simplifies the general approach.

Any continuous random vector variable $\mathbf{\Phi}$ taking real values $\boldsymbol{\phi} = (\phi_1, \ldots, \phi_m)$ can be completely specified by its probability density $P(\boldsymbol{\phi})$. Measure of the uncertainty (thus, measure of information) associated with the above random variable is named *Shannon differential entropy* $H[\mathbf{\Phi}]$ and reads [14]

$$H[\mathbf{\Phi}] = -\int_{supp\,\mathbf{\Phi}} P(\boldsymbol{\phi}) \log_2 P(\boldsymbol{\phi})\, d\boldsymbol{\phi}. \tag{1.1}$$

The *joint entropy* measures how much entropy is contained in a joint system of two random variables. If the random variables are $\mathbf{\Phi}$ and $\mathbf{\Psi}$, the joint entropy is written $H[\mathbf{\Phi}, \mathbf{\Psi}]$. Suppose, that each pair of possible outcomes is $(\boldsymbol{\phi}, \boldsymbol{\psi})$ which occurs with probability $P(\boldsymbol{\phi}, \boldsymbol{\psi})$, then the joint entropy is defined as

$$H[\mathbf{\Phi}, \mathbf{\Psi}] = -\int_{supp\,\{\mathbf{\Phi},\mathbf{\Psi}\}} P(\boldsymbol{\phi}, \boldsymbol{\psi}) \log_2 P(\boldsymbol{\phi}, \boldsymbol{\psi})\, d\boldsymbol{\phi}\, d\boldsymbol{\psi}.$$

Given two random variables $\mathbf{\Phi}$ and $\mathbf{\Psi}$ one can define a *conditional entropy* $H[\mathbf{\Phi}|\mathbf{\Psi}]$ which quantifies the remaining entropy (*i.e.* uncertainty) of a random variable $\mathbf{\Phi}$ given

that the value of another random variable $\mathbf{\Psi}$ is known:

$$H[\mathbf{\Phi}|\mathbf{\Psi}] = H[\mathbf{\Phi}, \mathbf{\Psi}] - H[\mathbf{\Psi}].$$

That allows to write down *mutual information* $I[\mathbf{\Phi} : \mathbf{\Psi}]$ measuring information shared between these variables as

$$I[\mathbf{\Phi} : \mathbf{\Psi}] = H[\mathbf{\Phi}] - H[\mathbf{\Phi}|\mathbf{\Psi}]. \tag{1.2}$$

Units for all entropies originated from Eq. (1.1) are *bits*.

This work mostly concerns probability densities which are m-variate Gaussian functions

$$P(\boldsymbol{\phi}) = \frac{1}{\sqrt{(2\pi)^m \det V}} \exp\left[-\frac{1}{2}\left(\boldsymbol{\phi} - \langle\boldsymbol{\phi}\rangle, V^{-1}\left(\boldsymbol{\phi} - \langle\boldsymbol{\phi}\rangle\right)\right)\right]$$

completely described by their vectors of mean values $\langle\boldsymbol{\phi}\rangle$ and covariance matrices V. Their differential entropy is

$$H[\mathbf{\Phi}] = \frac{1}{2}\ln\left[(2\pi e)^m \det V\right]. \tag{1.3}$$

1.2 Basics of quantum mechanics in phase space

Quantum mechanics in continuous variables can be introduced independently from Dirac approach as *Weyl star-product quantization* [15, 16] which operates with *symbols* (functions) defined on system phase space $(\mathbf{q}, \mathbf{p})$. *Quadratures* $\mathbf{q}$ and $\mathbf{p}$ are n-dimensional vectors of canonical variables. Below it will be useful to consider a vector

$$\mathbf{x} := (\mathbf{q}, \mathbf{p}) = (q_1, \ldots, q_n, p_1, \ldots, p_n). \tag{1.4}$$

In quantum optics systems variables $\mathbf{q}$ and $\mathbf{p}$ are fields $\mathbf{E}$ and $\mathbf{H}$, correspondingly. Any quantum state in this approach can be completely specified by its *Wigner function* $W(\mathbf{q}, \mathbf{p})$ [17] which is a Weyl symbol of density operator and whose relation with density matrix ρ in position representation for n-partite state reads[1]

$$\begin{aligned} W(\mathbf{q}, \mathbf{p}) &= \int \rho\left(\mathbf{q} + \frac{\mathbf{u}}{2}, \mathbf{q} - \frac{\mathbf{u}}{2}\right) e^{-i\mathbf{p}\mathbf{u}} d\mathbf{u}, \\ \rho(\mathbf{q}, \mathbf{q}') &= \frac{1}{(2\pi)^n} \int W\left(\mathbf{p}, \frac{\mathbf{q} + \mathbf{q}'}{2}\right) e^{i\mathbf{p}(\mathbf{q} - \mathbf{q}')} d\mathbf{p}. \end{aligned} \tag{1.5}$$

Quantum state ρ is called *Gaussian* if its Wigner function is Gaussian, therefore it is completely described by its quadratures covariance matrix V and vector $\mathbf{a}$ which represents quantum state displacement in phase space[2]:

$$\rho \;\longleftrightarrow\; W(\mathbf{x}) = \frac{1}{\sqrt{\det V}} \exp\left[-\frac{1}{2}\left(\mathbf{x} - \mathbf{a}, V^{-1}(\mathbf{x} - \mathbf{a})\right)\right]. \tag{1.6}$$

[1] Throughout this work it is assumed $\hbar = 1$.

[2] In what follows each Gaussian state and each (classical) Gaussian distribution are labelled by their quadratures covariance matrices, e.g. $\rho \leftrightarrow V$.

Throughout the paper the normalization of a n-mode Wigner function reads $\int W(\mathbf{x})\, d\mathbf{x} = (2\pi)^n$. In particular, $V = \mathrm{Id}_{2n}/2$ and $\mathbf{a} = \sqrt{2}\boldsymbol{\zeta}$ in Eq. (1.6) for n-partite coherent state of complex amplitude

$$\boldsymbol{\zeta} := (\boldsymbol{\zeta}_{\mathrm{R}}, \boldsymbol{\zeta}_{\mathrm{I}}) = (\mathrm{Re}(\zeta_1), \ldots, \mathrm{Re}(\zeta_n), \mathrm{Im}(\zeta_1), \ldots, \mathrm{Im}(\zeta_n)), \tag{1.7}$$

whose wave function is

$$\langle \mathbf{q}|\boldsymbol{\zeta}\rangle = \frac{1}{\pi^{n/4}} \exp\left(-\frac{\mathbf{q^2}}{2} + \sqrt{2}\,\mathbf{z}\,\mathbf{q} - \frac{\mathbf{z}^2}{2} - \frac{|\mathbf{z}|^2}{2}\right)$$

with $\mathbf{z} = (\zeta_1, \ldots, \zeta_n)$ and $\zeta_k = (q'_k + ip'_k)/\sqrt{2}$.

Below the relation between Wigner function and *Husimi function* [18]

$$P(\boldsymbol{\zeta}) = \frac{1}{\pi^n}\langle \boldsymbol{\zeta}|\rho|\boldsymbol{\zeta}\rangle \tag{1.8}$$

is used, which can be found as follows. Let us express the Husimi function through density matrix in position representation using orthogonal decomposition over position eigenstates, and then express that density matrix through Wigner function according to Eq. (1.5). This leads to the relation

$$\langle \boldsymbol{\zeta}|\rho|\boldsymbol{\zeta}\rangle = \frac{1}{(2\pi)^n} \int W\left(\frac{\mathbf{q}+\mathbf{q}'}{2}, \mathbf{p}\right) e^{i\mathbf{p}(\mathbf{q}-\mathbf{q}')} \langle \mathbf{q}'|\boldsymbol{\zeta}\rangle\langle\boldsymbol{\zeta}|\mathbf{q}\rangle\, d\mathbf{q}\, d\mathbf{p}\, d\mathbf{q}'. \tag{1.9}$$

By making the change of variables

$$\frac{\mathbf{q}+\mathbf{q}'}{2} \longrightarrow \mathbf{q}_1, \qquad \frac{\mathbf{q}-\mathbf{q}'}{2} \longrightarrow \mathbf{q}_2$$

in Eq. (1.9) and integrating it over the variable $\mathbf{q}_2$ one can get (see also [19]):

$$P(\boldsymbol{\zeta}) = \frac{1}{\pi^{2n}} \int W(\mathbf{x}) \exp\left[-(\mathbf{x} - \sqrt{2}\,\boldsymbol{\zeta})^2\right] d\mathbf{x}. \tag{1.10}$$

In particular, if $W(\mathbf{x})$ is a Gaussian state of the form (1.6) there is the following relation between quadratures covariance matrices in Wigner function and Husimi function:

$$V_{\mathrm{Husimi}} = V_{\mathrm{Wigner}} + \frac{1}{2}\,\mathrm{Id}_{2n}\,. \tag{1.11}$$

Note, that Heisenberg uncertainty relation (HUR) forbids quadratures to have joint probability density, but V_{Husimi} can be interpreted as the covariance matrix for a measurement in sense of *positive operator valued measure* (POVM) [20]. It is a measure whose values are non-negative self-adjoint operators on a Hilbert space $\mathcal{H}$ (in this thesis $L_2(\mathbb{R})$ is considered). In the simplest case, a POVM is a set of m Hermitian positive semidefinite operators $\{L_i\}$ on $\mathcal{H}$ that sum to unity:

$$\sum_{i=1}^{m} L_i = I_{\mathcal{H}}.$$

In the case of Husimi function (1.8) this sum is an integral over all complex variables ζ_j, with the corresponding POVM operators

$$L(\boldsymbol{\zeta}) = \bigotimes_{j=1}^{n} \frac{|\zeta_j\rangle\langle\zeta_j|}{\pi}. \tag{1.12}$$

Here $|\zeta_j\rangle$ is coherent state of jth mode having complex amplitude ζ_j. The POVM with operators (1.12) represents joint quadratures measurement and is often called *heterodyne measurement* [10, 21]. Analogously, the POVM operators

$$L(\boldsymbol{\zeta}) = \bigotimes_{j=1}^{n} |\operatorname{Re}\zeta_j\rangle\langle\operatorname{Re}\zeta_j| \tag{1.13}$$

represent a measurement of the single quadrature $\mathbf{q}/\sqrt{2} = \boldsymbol{\zeta}_{\mathrm{R}}$, and is often called *homodyne measurement* [10, 21].

As far as any quantum state must satisfy HUR there is a restriction on its quadratures covariance matrix V [22]:

$$V + i\Sigma \geqslant 0, \tag{1.14}$$

where $2n \times 2n$ *symplectic form* Σ is a commutation matrix for canonical variables (quadratures):

$$\Sigma = \begin{pmatrix} 0_n & \mathrm{Id}_n \\ -\mathrm{Id}_n & 0_n \end{pmatrix}.$$

Quantum mechanics makes phase space geometry symplectic, which allows to rewrite HUR in terms of *symplectic eigenvalues* $v_k(V)$ [22].

Definition: Numbers $v_k = v_k(V)$, $k = 1, \ldots, n$ are *symplectic eigenvalues* of covariance matrix

$$V = \begin{pmatrix} V_{qq} & V_{qp} \\ V_{qp}^{\top} & V_{pp} \end{pmatrix}, \text{ if } \pm i v_k \text{ are eigenvalues of } \widetilde{V} = \Sigma^{-1} V = \begin{pmatrix} -V_{qp}^{\top} & -V_{pp} \\ V_{qq} & V_{qp} \end{pmatrix}.$$

Then Eq. (1.14) can be rewritten as $v_k(V) \geqslant 1/2$, where equality is achieved only by pure states.

1.3 Von Neumann entropy of Gaussian state

Von Neumann entropy $S(\rho)$ (for quantum state ρ) extends concepts of classical Shannon entropy to the field of quantum mechanics [20]. By definition

$$S(\rho) := -\operatorname{Tr}(\rho \log_2 \rho). \tag{1.15}$$

It can be used as a measure of mixedness of quantum state as pure state has zero entropy. Let us calculate the von Neumann entropy for a Gaussian quantum state. Consider a thermal state with amount of N photons whose density operator ρ can be represented as a decomposition over Fock projectors:

$$\rho = \frac{1}{N+1} \sum_{m=0}^{\infty} \left(\frac{N}{N+1} \right)^m |m\rangle\langle m|. \tag{1.16}$$

Substituting this representation into Eq. (1.15) one can get that

$$S(\rho) = g(N),$$

where

$$g(x) := (x+1)\log_2(x+1) - x\log_2 x.$$

Properties of g-function are discussed in Appendix C. Operator (1.16) has a maximal entropy among all operators with restricted amount of photons N:

$$\mathrm{Tr}\left(\rho a^\dagger a\right) \leqslant N,$$

where a and $a^\dagger$ are ladder operators with commutation relation $[a, a^\dagger] = 1$ and photons number operator is $a^\dagger a$. Any Gaussian state can be transformed to thermal by applying *symplectic transformation* $\mathcal{S}$ to its quadratures covariance matrix [22]. This transformation is a map $V \to \mathcal{S}V\mathcal{S}^\top$ which does not change symplectic spectrum of V. Taking into account that symplectic eigenvalues v_j are related to amount of photons N_j for multimode state as [9]

$$v_j = N_j + \frac{1}{2},$$

and entropy is subadditive [20]:

$$S(\rho) = \sum_{j=1}^{n} S(\rho_j),$$

where n-modes thermal state is $\rho = \otimes_{j=1}^{n}\rho_j$, one can obtain von Neumann entropy for multimode thermal state:

$$S(\rho) = \sum_{j=1}^{n} g\left(v_k - \frac{1}{2}\right). \tag{1.17}$$

As symplectic transformation does not change symplectic spectrum, the relation (1.17) holds for any Gaussian state.

1.4 Gaussian quantum channels

Let us introduce main definitions from quantum channels theory [20]. *Positive map* is a linear map which maps input quantum states into output quantum states, *i.e.* preserves operator trace and its positivity. Positive map $\mathcal{T}$ is called *completely positive* if any map of the form $\mathcal{T} \otimes \mathrm{Id}$ is also positive. By definition, *quantum channel* T is that map which is completely positive. It can be sketched as follows:

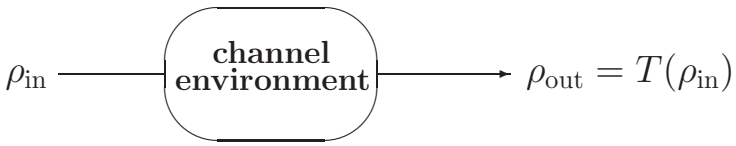

where ρ_{in} and ρ_{out} are density operators from input and output Hilbert spaces[3], correspondingly. *Stinespring's dilation theorem* allows any quantum channel T to be modelled

[3]In this thesis the dimensions of the input and the output Hilbert spaces coincide.

as interaction of the (input) system ρ_{in} with environment ρ_{env}:

$$\rho_{\text{out}} = T(\rho_{\text{in}}) = \text{Tr}_{\text{env}}[U(\rho_{\text{in}} \otimes \rho_{\text{env}})U^{\dagger}], \tag{1.18}$$

where ρ_{out} is quantum state of channel output, and unitary U specifies the action of the channel.

The channel $T^{\otimes n}$ which acts independently on each use is called *memoryless*. Otherwise, it is called *memory channel*. The environment state $\rho_{\text{env}}^{(n)}$ used to describe n uses of the memoryless channel can be represented as

$$\rho_{\text{env}}^{(n)} = \bigotimes_{k=1}^{n} \rho_{\text{env}}^{(1)},$$

where $\rho_{\text{env}}^{(1)}$ is the single-mode environment. Thus, the state $\rho_{\text{env}}^{(n)}$ can be interpreted as the environment for single use of n-mode channel.

Suppose that there are symbols $\{x\}$ belonging to a continuous alphabet, say $\mathbb{R}$, which are encoded into different quantum states $\{\rho_x\}$ at channel's input with some probability distribution $P(x)$. Then, at channel's output one can try to decode information by performing measurements on quantum states $\{\rho'_x\}$. This is what *classical information transmission* by quantum channels does:

$$\underset{\text{alphabet}}{\{x{\in}\mathbb{R}\}} \Longrightarrow \boxed{\underset{\text{input states}}{\{\rho_x\}}} \xrightarrow[\textbf{channel}]{\textbf{continuous}} \boxed{\underset{\text{output states}}{\rho'_x}} \Longrightarrow \underset{\text{measurement}}{\{L_y\}}$$

The aim at decoding (measurement of symbols y with the help of POVM operators L_y) is to distinguish states with different input symbols x. If that states are always perfectly distinguishable this is the case of ideal (noiseless) channel.

Achievable rate of information transmission is the speed[4] at which information can be reliably transferred through channel for fixed encoding and decoding. Formally it is the Shannon mutual information between the input X and output Y random variables. *Maximal achievable rate* of information transmission over channel (considering all possible types of encoding and decoding) is called *classical capacity*.

If electromagnetic fields E and H ("field quadratures") are taken as the continuous variables, the channel is called *bosonic*, as it operates with bosonic field modes. Achievable rates and capacity for bosonic channel are finite only if there is an *energy restriction* at channel input.

Gaussian channels are those bosonic channels which map Gaussian states into Gaussian states. Below only that quantum channels are considered which are both bosonic and Gaussian. If the symbols $\boldsymbol{\alpha}$ belonging to continuous complex alphabet are distributed with probability density $P(\boldsymbol{\alpha})$ in bosonic Gaussian channel, its average input state equals

$$\overline{\rho}_{\text{in}} = \int \rho_{\text{in}}^{(\boldsymbol{\alpha})} P(\boldsymbol{\alpha}) d\boldsymbol{\alpha},$$

[4]Amount of information per channel use can be interpreted as "speed".

and the average output state will be

$$\overline{\rho}_{\text{out}} = \int \rho_{\text{out}}^{(\boldsymbol{\alpha})} P(\boldsymbol{\alpha}) d\boldsymbol{\alpha} \equiv T\left[\overline{\rho}_{\text{in}}\right], \tag{1.19}$$

where $\rho_{\text{in}}^{(\boldsymbol{\alpha})}$ and $\rho_{\text{out}}^{(\boldsymbol{\alpha})}$ are quantum states of channel input and output, correspondingly, given classical symbol $\boldsymbol{\alpha}$.

Now suppose, that input state ρ_{in} is Gaussian of the form (1.6) with covariance matrix $V = V_{\text{in}}$ and displacement $\mathbf{a} = 0$. Also, let us assume that variable

$$\boldsymbol{\alpha} := (\boldsymbol{\alpha}_{\text{R}}, \boldsymbol{\alpha}_{\text{I}}) = (\text{Re}(\alpha_1), \ldots, \text{Re}(\alpha_n), \text{Im}(\alpha_1), \ldots, \text{Im}(\alpha_n)), \quad \alpha_j \in \mathbb{C} \tag{1.20}$$

is encoded via random displacement of ρ_{in} in phase space, that is

$$\rho_{\text{in}}^{(\boldsymbol{\alpha})} = \left[\otimes_{j=1}^{n} D_j(\alpha_j)\right] \rho_{\text{in}} \left[\otimes_{j=1}^{n} D_j(\alpha_j)\right]^{\dagger}, \tag{1.21}$$

where D_j denotes the displacement operator on the j-th mode [20]. Input state $\rho_{\text{in}}^{(\boldsymbol{\alpha})}$ is given by Eq. (1.6) in this case, where $V = V_{\text{in}}$ and $\mathbf{a} = \sqrt{2}\boldsymbol{\alpha}$.

If $\boldsymbol{\alpha}$ is chosen according to a Gaussian distribution

$$P(\boldsymbol{\alpha}) = \frac{1}{\pi^n \sqrt{\det V_{\text{cl}}}} \exp\left[-\left(\boldsymbol{\alpha}, V_{\text{cl}}^{-1}\boldsymbol{\alpha}\right)\right], \tag{1.22}$$

having classical covariance matrix $V_{\text{cl}}/2$, the covariance matrix of average input state reads

$$\overline{V}_{\text{in}} = V_{\text{in}} + V_{\text{cl}}. \tag{1.23}$$

The energy restriction can be represented in this case as

$$\frac{\text{Tr}\overline{V}_{\text{in}}}{2n} \leqslant N + \frac{1}{2}, \tag{1.24}$$

where N is average amount of photons per mode (per channel use). As output state of Gaussian channel is Gaussian, given Gaussian input state, the states ρ_{out} and $\overline{\rho}_{\text{out}}$ will be refered to by their quadratures covariance matrices V_{out} and $\overline{V}_{\text{out}}$, correspondingly.

1.5 Classical capacity

To evaluate the classical capacity one should maximize the mutual information overall possible encoding and decoding schemes, which seems an insurmountable task. Fortunately enough such evaluation always involves the so called Holevo χ quantity [23, 20].

The *Holevo* χ_n for n channel uses in the case of continuous alphabet distributed with probability density $P(\boldsymbol{\alpha})$ is defined through von Neumann entropy (1.15) as

$$\chi_n = S\left(\int \rho_{\text{out}}^{(\boldsymbol{\alpha})} P(\boldsymbol{\alpha}) d\boldsymbol{\alpha}\right) - \int S\left(\rho_{\text{out}}^{(\boldsymbol{\alpha})}\right) P(\boldsymbol{\alpha}) d\boldsymbol{\alpha}, \tag{1.25}$$

where $\rho_{\text{out}}^{(\boldsymbol{\alpha})}$ is a quantum state at the channel output. It represents an upper bound on the classical information that can be extracted from quantum channel output. *Coding*

theorem, suggested by J. P. Gordon [24] and later proved by A. S. Holevo [23, 25] and independently by B. Schumacher and M. D. Westmoreland [26], states that memoryless (one-shot) channel capacity is given by

$$C_1 = \max_{\rho_{\rm in},\rho_{\rm cl}} \chi_1,$$

where maximum is taken over all possible input states $\rho_{\rm in}$ satisfying the energy constraint and classical alphabet distributions $\rho_{\rm cl}$. The full (*regularized*) capacity is then obtained as[5]

$$C = \lim_{n\to\infty} \frac{1}{n} \max_{\rho_{\rm in},\rho_{\rm cl}} \chi_n.$$

If consideration is not restricted to memoryless channels, one can define the following bounds on the regularized classical capacity [A4,A5]:

$$\overline{C} := \lim_{n\to\infty} \overline{C}_n; \quad \overline{C}_n = \frac{1}{n} \max_{\rho_{\rm in},\rho_{\rm cl}} \chi_n, \tag{1.26}$$

and

$$\underline{C} := \lim_{n\to\infty} \underline{C}_n; \quad \underline{C}_n = \frac{1}{n} \max_{V_{\rm in},V_{\rm cl}} \chi_n, \tag{1.27}$$

where the maximum is taken over set of Gaussian states $V_{\rm in}$ and Gaussian distributions $V_{\rm cl}$. The bound (1.26) comes directly from the definition of the Holevo-χ quantity as an upper bound on the accessible information. The bound (1.27) comes from the following reasoning: for any n, one can look at n uses of the channel as a single channel acting on n modes. Then by considering the channel memoryless form n uses to another n uses, one can exploit the lower bound on the classical capacity of memoryless channels computed by maximizing the one-shot capacity over Gaussian input states and Gaussian distributions for encoding of classical symbols. In the case of memoryless bosonic Gaussian channels with vacuum environment it turns out that [11]

$$C = \overline{C} = \underline{C} = C_1,$$

but the above equalities are conjectures in the case of arbitrary bosonic memoryless Gaussian channels.

The Holevo-χ quantity for Gaussian states reads (see Eqs. (1.17) and (1.25)) [8]:

$$\chi_n = \sum_{k=1}^{n} \left[g\left(\overline{\nu}_k - \frac{1}{2}\right) - g\left(\nu_k - \frac{1}{2}\right) \right], \tag{1.28}$$

where $\overline{\nu}_k$ and ν_k are the symplectic eigenvalues of $\overline{V}_{\rm out}$ and $V_{\rm out}$, respectively. Thus, one can state the optimization problem of finding the classical capacity as searching matrices $V_{\rm in}, V_{\rm cl}$ satisfying energy constraint (1.24), such as $V_{\rm cl} \geqslant 0$ and $V_{\rm in} + i\Sigma \geqslant 0$, thus giving the maximum of Eq. (1.27).

[5]The dimension of quantum states $\rho_{\rm in}$ and (classical) distributions $\rho_{\rm cl}$ is taken in a way to correspond to dimension of χ_n, given n is chosen.

Chapter 2

Lossy bosonic memory channel

In this chapter the notion of lossy bosonic memory channel (LBMC) is introduced, and the relations for capacity and rates as functions of covariance matrices are presented (following [A1]).

2.1 Definitions

The single-mode lossy bosonic channel (LBC) is sketched on Fig. 2.1. Input mode (state) $V_{\rm in}$ interacts with environment mode (state) $V_{\rm env}$ through a beam-splitter (BS) with transmissivity η. The total state of the system "input+environment" before interaction is taken in the form $V_{\rm tot}^{\rm (in)} = V_{\rm in} \oplus V_{\rm env}$. BS unitary action (see general relation (1.18)) can be represented as the transformation of input and environment quadratures:

$$\begin{aligned} q^{\rm (in)} &\to \sqrt{\eta}\, q^{\rm (in)} + \sqrt{1-\eta}\, q^{\rm (env)}, \\ p^{\rm (in)} &\to \sqrt{\eta}\, p^{\rm (in)} + \sqrt{1-\eta}\, p^{\rm (env)}, \\ q^{\rm (env)} &\to -\sqrt{1-\eta}\, q^{\rm (in)} + \sqrt{\eta}\, q^{\rm (env)}, \\ p^{\rm (env)} &\to -\sqrt{1-\eta}\, p^{\rm (in)} + \sqrt{\eta}\, p^{\rm (env)}, \end{aligned} \tag{2.1}$$

which relate output state of the channel with its input and environment as

$$V_{\rm out} = \eta\, V_{\rm in} + (1-\eta)\, V_{\rm env}. \tag{2.2}$$

In particular, averaged over encoding input state $\overline{V}_{\rm in}$ (see Eq. (1.23)) gives average output state[1]

$$\overline{V}_{\rm out} = \eta\, (V_{\rm in} + V_{\rm cl}) + (1-\eta)\, V_{\rm env}. \tag{2.3}$$

Let us now consider the classical use of LBC where input quantum states carry the values of a random classical variable. Channel mapping $\rho \mapsto T[\rho]$ then can be seen as a mapping of phase space points, therefore two real random values (or one complex) for each mode are carried. An input state is labelled as $\rho_{\rm in}^{(\boldsymbol{\alpha})}$ with classical variable $\boldsymbol{\alpha}$ distributed according to Eq. (1.22) and encoded via random displacements of a suitable

[1] One can show that output state averaged over encoding is the same as output state corresponding to averaged input state, therefore these cases are not distinguished in this thesis.

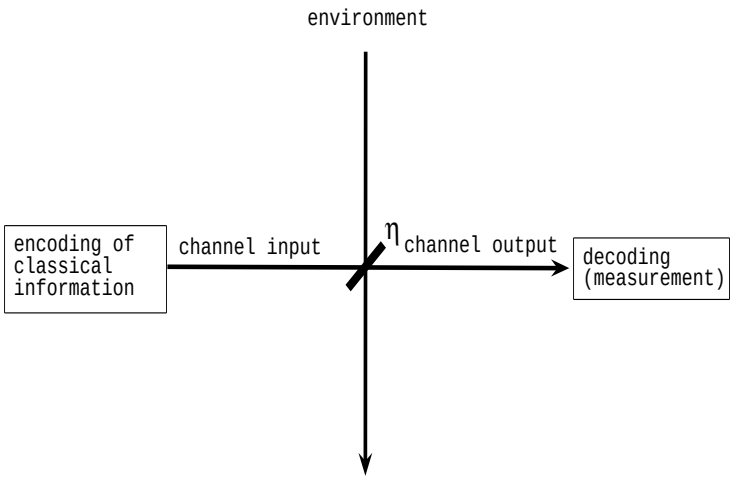

Figure 2.1: Single use of lossy bosonic channel. Input mode interacts with environment mode through beam-splitter with transmissivity η.

(Gaussian) seed state $\rho_{\rm in}$ (see Eqs. (1.20) and (1.21)). The Wigner function of the system "input+environment" is given in this case by Eq. (1.6) after the formal substitution $V \to V_{\rm tot}^{\rm (in)}$, $\mathbf{x} \to \mathbf{x}_{\rm tot}$ and $\mathbf{a} \to \sqrt{2}\boldsymbol{\alpha}_{\rm tot}$, where[2] $\mathbf{x}_{\rm tot} := (\mathbf{x}_{\rm in}, \mathbf{x}_{\rm env})$ and $\boldsymbol{\alpha}_{\rm tot} := (\boldsymbol{\alpha}, 0)$. By applying BS unitary transformation $\mathbf{x}_{\rm tot} \to B\mathbf{x}_{\rm tot}$ in this Wigner function with the block matrix

$$B = \begin{pmatrix} \sqrt{\eta}\,\mathrm{Id}_{2n} & \sqrt{1-\eta}\,\mathrm{Id}_{2n} \\ -\sqrt{1-\eta}\,\mathrm{Id}_{2n} & \sqrt{\eta}\,\mathrm{Id}_{2n} \end{pmatrix},$$

and then integrating over the environment variables $\mathbf{x}_{\rm env}$, one can arrive at the output state Wigner function

$$W_{\rm out}^{(\boldsymbol{\alpha})}(\mathbf{x}_{\rm out}) = \frac{1}{\sqrt{\det V_{\rm out}}} \exp\left[-\frac{1}{2}\left(\mathbf{x}_{\rm out} - \sqrt{2\eta}\,\boldsymbol{\alpha}, V_{\rm out}^{-1}\left(\mathbf{x}_{\rm out} - \sqrt{2\eta}\,\boldsymbol{\alpha}\right)\right)\right]. \tag{2.4}$$

Analogously, one can show that the average output state (1.19) will be characterized by the Wigner function with covariance matrix (2.3).

Let us now introduce memory effects in LBC. This can be done by considering multimode states for input and environment of the channel and allowing correlations among them. The model of LBMC T is depicted in Fig.2.2. Each use of the channel corresponds to its own input mode. n of such modes (uses) with corresponding environment modes, which interact through beam splitters with (the same) transmittivity η, are considered. The interaction leads to the transformations (2.1) written for each mode. All the above relations (including Eqs. (2.2) and (2.3)) for multimode case are the same as for a single mode, but with higher dimension.[3]

For a (multimode) memoryless channel, the environment modes are initially in an uncorrelated state, the vacuum state in the simplest case. The classical capacity is achieved in this case by using $\rho_{\rm in} = |0\rangle\langle 0|^{\otimes n}$ and $V_{\rm cl} = \mathrm{diag}(N)$, where N is the average number

[2]The indexes "in" and "env" denote quadratures (1.4) related to proper states' space.

[3]Their generalization from a single mode to multimode channel is strightforward, therefore it is not discussed here in detail.

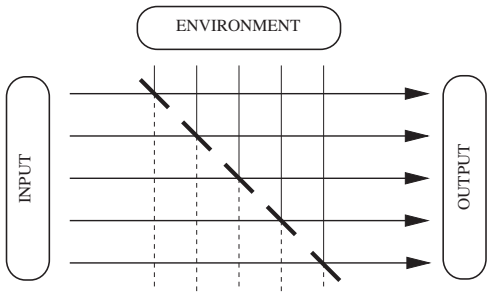

Figure 2.2: The model for a lossy bosonic channel T. Each input mode (left-right line), representing one use of the channel, interacts with the corresponding environment mode (top-bottom line) through a beam-splitter. To introduce memory effects, environment modes are initially considered in a correlated state.

of input photons per mode [11]. In such a case squeezed (correlated) inputs turn out to not be useful. More generally, below a Gaussian state characterized by zero displacement vector and covariance matrix $V_{\rm env}$ correlated among channel uses will be considered.

2.2 Memory model

It is reasonable to consider a model of channel's environment which allows analytical investigation of both capacity and rates. Symplectic eigenvalues of covariance matrix are not functions of matrix spectrum in general. However, to simplify the problem the case of symplectic spectrum being function of (usual) spectrum will be considered. In the simplest case this means to restrict the environment's covariance matrices to those of the form

$$V_{\rm env} = \begin{pmatrix} V_{\rm env}^{(qq)} & 0 \\ 0 & V_{\rm env}^{(pp)} \end{pmatrix} \tag{2.5}$$

with commuting blocks $V_{\rm env}^{(qq)}$ and $V_{\rm env}^{(pp)}$. Such a matrix can be diagonalized by means of transformation which is orthogonal and symplectic at the same time, *i.e.* it preserves matrix trace and symplectic eigenvalues [22].

Note, that symplectic eigenvalue is always a spectrum function for a single mode matrix $V_{\rm env}$, which is equal to $\sqrt{\det V_{\rm env}}$. This will allow us to consider environment mode in the most general Gaussian form for capacity investigation. It was shown in [27] for a single use noisy channel[4] that matrices $V_{\rm env}$, $V_{\rm in}$ and $V_{\rm cl}$ maximizing Holevo χ should commute each with other. This was done by applying Lagrange multipliers method and taking into account input purity theorem discussed below in page 23. Generalization of this result to capacity and rates in LBC is strightforward.

As concerns multimode case, this commutation property is taken as a conjecture in this thesis. It is also conjectured that the maximum of χ-quantity (1.28) and rates is achieved with matrices $V_{\rm in}$ and $V_{\rm cl}$ of the same form as (2.5), *i.e.* with null off-diagonal blocks. Furthermore, all diagonal blocks of all matrices are assumed to be mutually commuting. These conjectures are supported by numerical investigations relying on environment models of the form (2.5).

[4]Noisy channel is described by the relations $V_{\rm out} = V_{\rm in} + V_{\rm env}$ and $\overline{V}_{\rm out} = V_{\rm in} + V_{\rm cl} + V_{\rm env}$ analogous to Eqs. (2.2) and (2.3).

Below the eigenvalues of matrices $V_{\rm in}$, $V_{\rm env}$, $V_{\rm out}$, $V_{\rm cl}$ and $\overline{V}_{\rm out}$ will be refered to as i_{uk}, e_{uk}, o_{uk}, c_{uk} and a_{uk} respectively. Since $n \in \mathbb{N}$ represents the number of bosonic modes (channel uses), the dimension of all above matrices is $2n \times 2n$ and $k = 1, \ldots, n$, while u denotes either quadrature q or p (if $u = q$, then $u_\star = p$, and vice versa). In particular, taking into account the above conjectures, LBMC gives rise to the following relations among eigenvalues of matrices:

$$\begin{aligned} o_{uk} &= \eta\, i_{uk} + (1-\eta) e_{uk}, \\ a_{uk} &= \eta(i_{uk} + c_{uk}) + (1-\eta) e_{uk}. \end{aligned} \tag{2.6}$$

As a consequence, the following expressions take place for symplectic eigenvalues:

$$\nu_k = \sqrt{o_{qk} o_{pk}}, \qquad \overline{\nu}_k = \sqrt{a_{qk} a_{pk}}. \tag{2.7}$$

Notice, that both energy constraint (1.24) and symplectic spectrum (2.7) are preserved under orthogonal transformations. Thus, without affecting the final result, below all the involved matrices are considered to be diagonal (see also the discussion in the appendix of [A4]).

2.3 Conventional decodings

Let us now consider information transmission rates for LBMC by conventional decoding procedures like heterodyne (1.12) and homodyne (1.13) measurements.

For the case of heterodyne measurement, the probability (1.8) of the output coherent amplitudes $\boldsymbol{\zeta}$ is related to the probability (2.4) for the corresponding quadratures $\mathbf{x}_{\rm out}$ by means of the relation (1.11). Thus, the conditional probability of getting $\boldsymbol{\zeta}$ at the output given the encoded $\boldsymbol{\alpha}$ at input results

$$P(\boldsymbol{\zeta}|\boldsymbol{\alpha}) = \frac{1}{\pi^n \sqrt{\det V_{\zeta|\alpha}}} \exp\left[- \left(\boldsymbol{\zeta} - \sqrt{\eta}\, \boldsymbol{\alpha}, V_{\zeta|\alpha}^{-1} \left(\boldsymbol{\zeta} - \sqrt{\eta}\, \boldsymbol{\alpha} \right) \right) \right], \tag{2.8}$$

where

$$V_{\zeta|\alpha} := V_{\rm out} + \frac{1}{2} \mathrm{Id}_{2n}$$

is the relation for quadratures' covariance matrices. Here, the term $1/2$ represents the quadrature vacuum noise added by heterodyne measurement.

For the case of homodyne measurement one should consider information only encoded in $\boldsymbol{\alpha}_R$ (see Eq. (1.20)). Hence, while keeping the usual energy constraint, the matrix $V_{\rm cl}$ in Eq. (1.22) can be written as

$$V_{\rm cl} = \begin{bmatrix} V_{\rm cl}^{(qq)} & 0 \\ 0 & 0 \end{bmatrix}.$$

Taking into account that the random variables $\boldsymbol{\alpha}_R$ and $\boldsymbol{\zeta}_R$ are independent from $\boldsymbol{\alpha}_I$ and $\boldsymbol{\zeta}_I$ in the output Wigner function (2.4), by integrating it over $\boldsymbol{\zeta}_I$ one can get $P(\boldsymbol{\zeta}_R|\boldsymbol{\alpha}_R)$. Its expression results like (2.8) with the replacements $n \to n/2$, $V_{\zeta|\alpha} \to V_{\rm out}^{(qq)}$, $\boldsymbol{\zeta} \to \boldsymbol{\zeta}_R$ and $\boldsymbol{\alpha} \to \boldsymbol{\alpha}_R$.

Similarly to (2.8), Eqs. (1.19) and (2.3) yield the output probability for the heterodyne case

$$P(\boldsymbol{\zeta}) = \frac{1}{\pi^n \sqrt{\det V_\zeta}} \exp\left[-\left(\boldsymbol{\zeta}, V_\zeta^{-1}\boldsymbol{\zeta}\right)\right], \tag{2.9}$$

where

$$V_\zeta := \overline{V}_{\text{out}} + \frac{1}{2}\,\text{Id}_{2n}\,.$$

In the same fashion, one can get the output probability for the homodyne case $P(\boldsymbol{\zeta}_R)$ by integrating over $\boldsymbol{\zeta}_I$ the averaged output Wigner function. Its expression results like (2.9) with the replacements $n \to n/2$, $V_\zeta \to \overline{V}^{(qq)}_{\text{out}}$ and $\boldsymbol{\zeta} \to \boldsymbol{\zeta}_R$.

Applying the definition (1.2) to Eqs. (2.8) and (2.9), and taking into account Eq. (1.3) one can arrive at the mutual information for heterodyne case [A1][5]

$$I[\boldsymbol{Z} : \boldsymbol{A}] = \frac{1}{2}\log_2 \det\left[\left(\overline{V}_{\text{out}} + \frac{1}{2}\,\text{Id}_{2n}\right)\left(V_{\text{out}} + \frac{1}{2}\,\text{Id}_{2n}\right)^{-1}\right]. \tag{2.10}$$

Analogously, for the homodyne case it can be found [A1]

$$I[\text{Re}\,\boldsymbol{Z} : \text{Re}\,\boldsymbol{A}] = \frac{1}{2}\log_2 \det\left[\left(\overline{V}^{(qq)}_{\text{out}}\right)\left(V^{(qq)}_{\text{out}}\right)^{-1}\right]. \tag{2.11}$$

Considering average information accessible from single channel use and asymptotic behavior of the channel one can get heterodyne rate

$$F^{(\text{het})} := \lim_{n\to\infty} F_n^{(\text{het})}; \quad F_n^{(\text{het})} = \frac{1}{2n}\max_{V_{\text{in}},V_{\text{cl}}} \log_2 \det\left[\left(\overline{V}_{\text{out}} + \frac{1}{2}\,\text{Id}_{2n}\right)\left(V_{\text{out}} + \frac{1}{2}\,\text{Id}_{2n}\right)^{-1}\right] \tag{2.12}$$

and homodyne (measurement of u-quadratures) rate

$$F^{(\text{hom})} := \lim_{n\to\infty} F_n^{(\text{hom})}; \quad F_n^{(\text{hom})} = \frac{1}{2n}\max_{V_{\text{in}},V_{\text{cl}}} \log_2 \det\left[\left(\overline{V}^{(uu)}_{\text{out}}\right)\left(V^{(uu)}_{\text{out}}\right)^{-1}\right]. \tag{2.13}$$

2.4 Input purity theorem

Let us formulate optimization problems for classical capacity and rates in the case of memory model (2.5). One can note from Eqs. (1.28), (2.12) and (2.13) that both rates and capacity are monotonicaly growing functions of c_{uk}. It means that one needs to consider equality in energy constraint (1.24). That is also evident from physical point of view: capacity and rates are monotonicaly growing functions of N.

Taking into account all constraints for n channel uses (energy restriction, positivity and HUR), the main problem implies finding of eigenvalues i_{uk}, c_{uk}, such as

$$\frac{1}{2n}\sum_{k=1}^{n}\left[i_{uk} + i_{u^\star k} + c_{uk} + c_{u^\star k}\right] = N + \frac{1}{2}, \quad i_{uk} > 0, \quad c_{uk} \geqslant 0, \quad i_{uk} i_{u^\star k} \geqslant \frac{1}{4},$$

[5]Recall, that this expression has been obtained by exploiting the commutativity of covariance matrices.

which give a maximum to functions χ_n/n, $I[\boldsymbol{Z}:\boldsymbol{A}]/n$ and $I[\mathrm{Re}\,\boldsymbol{Z}:\mathrm{Re}\,\boldsymbol{A}]/n$. After that one need to take the limit $n\to\infty$ for the solution found. These maximization problems can be simplified taking into account the following [27]:

> Theorem: Suppose, there is the case of LBMC with all covariance matrices to be diagonal, then the maximum of Holevo bound is always achieved on pure input state: $i_{uk}i_{u_\star k}=\frac{1}{4}$.

Proof: Suppose, that the maximum of the Holevo bound is achieved by $i_{uk}i_{u_\star k}>1/4$. This means that some real numbers $\delta_k>0$ exist, such that $i_{u_\star k}=i'_{u_\star k}+\delta_k$, where $i'_{u_\star k}=1/(4i_{uk})$. Let us change variables to make V_{in} pure (it preserves energy constraint N):

$$\begin{aligned} i'_{u_\star k}&=i_{u_\star k}-\delta_k, & i'_{uk}&=i_{uk},\\ c'_{u_\star k}&=c_{u_\star k}+\delta_k, & c'_{uk}&=c_{uk}. \end{aligned}$$

These new variables (denoted with primes) lead to $\overline{\nu}'_k=\overline{\nu}$ and $\nu'_k<\nu_k$. As far as g is monotonically growing function of its argument, the Holevo bound calculated for new variables will be higher:

$$C_k(i'_{uk},i'_{u_\star k},c'_{uk},c'_{u_\star k})>C_k(i_{uk},i_{u_\star k},c_{uk},c_{u_\star k}),$$

where C_k is the contribution of k-th mode to capacity (see Eqs. (1.27) and (1.28)):

$$\underline{C}_n=\frac{1}{n}\sum_{k=1}^{n}C_k,\quad C_k=g\left(\overline{\nu}_k-\frac{1}{2}\right)-g\left(\nu_k-\frac{1}{2}\right). \tag{2.14}$$

It means, that initial (non pure) eigenvalues i_{uk} did not give the maximum of χ_n. Hence, the theorem is proved by contradiction. ■

The extension of this theorem to the case of rates is strightforward. Thus, one can exclude variable $i_{u_\star k}$ from the optimization problem, and positivity of eigenvalues are the only inequalities to retain among constraints. It will allow us in next chapter to apply standard Lagrange multipliers method to find the maximums $\underline{C}_n$, $F_n^{(\mathrm{het})}$ and $F_n^{(\mathrm{hom})}$.

2.5 Capacity and rates

By applying Eq. (4.24) to (1.28) one can get, at lowest order,

$$\chi_n^{(0)}=\sum_{k=1}^{n}\log_2\frac{\overline{\nu}_k}{\nu_k}, \tag{2.15}$$

which (after dividing by n) gives the zeroth-order approximation to lower bound[6] on classical capacity $\underline{C}_n^{(0)}$. It is interesting to notice that the following relation takes place (see Eqs. (2.7)):

$$F_n^{(\mathrm{hom})}=\underline{C}_n^{(0)}, \tag{2.16}$$

[6]Below the words "lower bound" will be often omitted.

for the case of zero eigenvalues corresponding to q- or p-quadratures[7] ($c_{uk} = 0$, $\forall k$), *i.e.* the homodyne rate coincides with the capacity at zeroth-order approximation.

Analogously, for heterodyne measurement it is

$$F_n^{(\mathrm{het})} = \frac{1}{n}\sum_{k=1}^{n} \log_2 \frac{\overline{\nu}_k^{(\mathrm{het})}}{\nu_k^{(\mathrm{het})}},$$

where $\overline{\nu}_k^{(\mathrm{het})}$ and $\nu_k^{(\mathrm{het})}$ are symplectic eigenvalues of $\overline{V}_{\mathrm{out}}$ and V_{out} calculated by using *(heterodyne) modified environment matrix*

$$V_{\mathrm{env}}^{(\mathrm{het})} = V_{\mathrm{env}} + \frac{1}{2(1-\eta)}\,\mathrm{Id}_{2n}\,.$$

Thus, the heterodyne rate is equal to the zeroth-order approximation of capacity calculated with $V_{\mathrm{env}}^{(\mathrm{het})}$. In the following it will be useful to introduce the *average amount of photons in environment* M_{env} ($M_{\mathrm{env}}^{(\mathrm{het})}$ for the modified environment) according to the relations

$$\frac{\mathrm{Tr}V_{\mathrm{env}}}{2n} = M_{\mathrm{env}} + \frac{1}{2}, \qquad \frac{\mathrm{Tr}V_{\mathrm{env}}^{(\mathrm{het})}}{2n} = M_{\mathrm{env}}^{(\mathrm{het})} + \frac{1}{2}.$$

Furthermore, the eigenvalues of the matrix $V_{\mathrm{env}}^{(\mathrm{het})}$ will be denoted by

$$e_{uk}^{(\mathrm{het})} = e_{uk} + \frac{1}{2(1-\eta)}, \qquad e_{u_\star k}^{(\mathrm{het})} = e_{u_\star k} + \frac{1}{2(1-\eta)}. \tag{2.17}$$

Similarly, the notations for the other eigenvalues are

$$\begin{aligned} a_{uk}^{(\mathrm{het})} &= a_{uk} + \frac{1}{2}, & o_{uk}^{(\mathrm{het})} &= o_{uk} + \frac{1}{2}, \\ a_{u_\star k}^{(\mathrm{het})} &= a_{u_\star k} + \frac{1}{2}, & o_{u_\star k}^{(\mathrm{het})} &= o_{u_\star k} + \frac{1}{2}. \end{aligned} \tag{2.18}$$

For the single-mode environment matrices V_{env} and $V_{\mathrm{env}}^{(\mathrm{het})}$ can be represented as

$$V_{\mathrm{env}} = \left(N_{\mathrm{env}} + \frac{1}{2}\right)\begin{bmatrix} e^{s} & 0 \\ 0 & e^{-s} \end{bmatrix}, \tag{2.19}$$

$$V_{\mathrm{env}}^{(\mathrm{het})} = \left(N_{\mathrm{env}}^{(\mathrm{het})} + \frac{1}{2}\right)\begin{bmatrix} e^{s_{\mathrm{het}}} & 0 \\ 0 & e^{-s_{\mathrm{het}}} \end{bmatrix}, \tag{2.20}$$

where N_{env} ($N_{\mathrm{env}}^{(\mathrm{het})}$) is amount of *environment thermal photons* and s (s_{het}) is the *environment squeezing parameter*. They are related as

$$\begin{aligned} M_{\mathrm{env}}^{(\mathrm{het})} &= M_{\mathrm{env}} + \frac{1}{2(1-\eta)}, \\ \left(N_{\mathrm{env}}^{(\mathrm{het})} + \frac{1}{2}\right)^2 &= \left(N_{\mathrm{env}} + \frac{1}{2} + \frac{1}{2(1-\eta)}\right)^2 + \frac{M_{\mathrm{env}} - N_{\mathrm{env}}}{1-\eta}. \end{aligned} \tag{2.21}$$

[7] Quadratures $u_\star$ measured for homodyne rate have to correspond to optimal non-zero quadratures $c_{u_\star k}$ for $\chi_n^{(0)}$.

In this case one can get for a fixed s

$$\lim_{N_{\rm env}\to\infty} F_n^{(\rm het)} = \underline{C}_n^{(0)}. \tag{2.22}$$

Eqs. (2.16) and (2.22) define the values of parameters s and $N_{\rm env}$ for which the rates approach[8] the capacity (see also discussion in [11]).

2.6 Open problems and conjectures

There are open problems directly related with the results obtained in this chapter. Their solution could extend the meaning and applicability of these results to a wider set of problems. Here a list of these problems is given.

1. The relations (2.10) and (2.11) were obtained for matrices of the form (2.5) taking into account mutual commutation of all blocks in matrices $V_{\rm in}$, $V_{\rm cl}$ and $V_{\rm env}$. Extension of these relations to the case of arbitrary covariance matrices is not known.

2. Homodyne rate (2.13) corresponds to the case of measurement of the same quadrature (q or p) in all modes. It could be extended to the case of measurement of different quadratures for different modes, at first, and to measurement of quadratures rotated in phase space, at second. The last one could make useful the methods of optical [28] and symplectic [29, 30] tomography.

3. The model (2.5) relies on $V_{\rm in}$ and $V_{\rm cl}$ of the same form as (2.5), *i.e.* on matrices with zero equal off-diagonal blocks, where all diagonal blocks mutually commute. An optimality of such a choice (for multimode case) for capacity and rates is not shown.

Conjectures about future possible results:

1. The relation for a heterodyne rate (2.12) is valid for arbitrary matrices $V_{\rm in}$, $V_{\rm cl}$ and $V_{\rm env}$, *i.e.* not necessarily of the form (2.5).

2. The consideration of quadratures' rotation in phase space will not give higher homodyne rate than (2.13) for the model (2.5). This is expected because optimal homodyne measurement should correspond to measurement of quadratures with less noise. As far as the model (2.5) finally operates with only diagonal matrices, the above homodyne measurement should be optimal.

These open problems and conjectures could inspire futher investigations in this area.

[8] Finding the type of encoding and decoding which allow to achieve the capacity is one of the main difficulties in quantum information theory, but this problem is not discussed in detail in this thesis.

Chapter 3

Solution for the optimization problem

The general solution of optimization problem (along with [A5]) which allows to find capacity and rates is given in this chapter. A single channel use for both single-mode (the case of LBC) and multimode (the case of LBMC) channels is considered for arbitrary model of the form (2.5).

Note, that despite the relation (1.28) for Holevo χ is valid for the matrices $V_{\rm in}$, $V_{\rm cl}$ and $V_{\rm env}$ of general form, the relations for rates (2.12) and (2.13) are known only if these matrices are diagonal. However, since the matrix $V_{\rm env}$ for arbitrary single-mode channel and for multimode channel with environment model (2.5) can always be taken in diagonal form, it is conjectured that besides capacity also rates do not depend on orthogonal transformation. Thus, below all the matrices are assumed to be diagonal without loss of generality. For the sake of simplicity each function to maximize will be denoted by the same character as its proper maximum.

3.1 Single-mode use: memoryless case

Let us consider single use of single-mode LBC. Its capacity and rates are the same as for n uses of the corresponding n-mode memoryless channel. As far as only the single-mode case is discussed, index k (see Eqs. (2.6) and (2.7)) is omitted for all eigenvalues.

3.1.1 Solution of Lagrange equations

The optimization problem for single-mode channel can be formulated as follows. One needs to find the maximum over the variables i_u, c_u, and $c_{u_\star}$ for the following functions:

$$\underline{C} = g\left(\overline{\nu} - \frac{1}{2}\right) - g\left(\nu - \frac{1}{2}\right), \tag{3.1}$$

$$F^{(\rm het)} = \log_2 \overline{\nu}^{(\rm het)} - \log_2 \nu^{(\rm het)}, \tag{3.2}$$

$$F^{(\rm hom)} = \frac{1}{2}\left(\log_2 a_{u_\star} - \log_2 o_{u_\star}\right) \tag{3.3}$$

with the constraints[1]

$$\begin{aligned} & i_u > 0 \\ & c_u, c_{u_\star} \geqslant 0 \\ & i_u + \frac{1}{4i_u} + c_u + c_{u_\star} = 2N + 1. \end{aligned} \tag{3.4}$$

Below it will be shown that all solutions of Lagrange equations give positive i_u, *i.e.* $c_u, c_{u_\star} \geqslant 0$ are the only inequalities to satisfy. One can classify all solutions depending on the amount of positive c-quadratures. The following terminology is used for this purpose.

Definition: The solution belongs to the *first stage* if both $c_u, c_{u_\star} = 0$, to the *second stage* if only single c-quadratrure equals zero, and to the *third stage* if $c_u, c_{u_\star} > 0$.

As far as $F^{(\mathrm{hom})}$ does not depend on c_u, due to the condition (3.4) the maximum is achieved for $c_u = 0$ which shows the absence of the third stage in homodyne rate. In other words, energy N should not be wasted in the quadrature not used for information transmission.

The first stage holds if and only if capacity and rates equal zero, which can be only if $N = 0$ (if $N \neq 0$ one can always get non-zero capacity and rates by taking $i_u = 1/2$, $c_u = c_{u_\star} = N$). In particular, Eq. (3.4) applied for the first stage gives $i_u = 1/2$.

Below it is always assumed for non-equal environment eigenvalues that $e_u > e_{u_\star}$.

Proposition: If $e_u > e_{u_\star}$, then optimal $c_u = 0$ but never $c_{u_\star} = 0$ in the second stage.

Proof: Suppose that $c_{u_\star} = 0$. The energy constraint (3.4) is preserved by variables change $c'_u = c'_{u_\star} = c_u/2$, $i'_u = i_u$. New variables do not change the second terms in Eqs. (3.1) and (3.2) but increase the first terms[2]. Thus, new variables give higher capacity and heterodyne rate. The above statement is proved by contradiction. ■ Analogously, one can prove that

$$o_u > a_{u_\star} > o_{u_\star} \tag{3.5}$$

in the second stage.

The similar consideration gives $a_u = a_{u_\star}$ in the third stage (by supposing $a_u \neq a_{u_\star}$ one can always find such redistribution of energy N among c-quadratures which decreases the difference $|a_u - a_{u_\star}|$ thus giving higher capacity and heterodyne rate). Taking into account Eq. (3.4) in this case

$$a_u = a_{u_\star} = \eta \left(N + \frac{1}{2} \right) + (1 - \eta) \left(M_{\mathrm{env}} + \frac{1}{2} \right). \tag{3.6}$$

Below the solutions for the third and the second stages are presented.

[1] See definitions (2.6) and remember that $i_{u_\star} = 1/(4i_u)$.

[2] Area of rectangle with fixed perimeter is higher if lenths of sides differs less. In the considered case $a'_u + a'_{u_\star} = a_u + a_{u_\star}$ but $|a'_u - a'_{u_\star}| < |a_u - a_{u_\star}|$. Then, both g and $\log_2$ are monotonic functions.

The third stage

In the case of the third stage Lagrange multipliers method applied to the function $\underline{C}$ with the constraint (3.4) leads to the following system of equations (see definitions of g_k in (4.26)):

$$\frac{\partial L}{\partial i_u} = \frac{\eta}{2}\left[g_1(\overline{\nu})\left(\frac{1}{a_u} - \frac{1}{4i_u^2 a_{u_\star}}\right) - g_1(\nu)\left(\frac{1}{o_u} - \frac{1}{4i_u^2 o_{u_\star}}\right)\right] - \lambda\left[1 - \frac{1}{4i_u^2}\right] = 0, \tag{3.7}$$

$$\frac{\partial L}{\partial c_u} = \frac{\eta}{2}\frac{g_1(\overline{\nu})}{a_u} - \lambda = 0, \tag{3.8}$$

$$\frac{\partial L}{\partial c_{u_\star}} = \frac{\eta}{2}\frac{g_1(\overline{\nu})}{a_{u_\star}} - \lambda = 0, \tag{3.9}$$

where the Lagrange function is

$$L = \underline{C} - \lambda\left(i_u + \frac{1}{4i_u} + c_u + c_{u_\star} - 2N - 1\right).$$

The heterodyne rate results in the same system of equations (3.7)-(3.9) with the replacements $g_1 \to 1/\ln 2$, $a_u \to a_u^{(\mathrm{het})}$, $a_{u_\star} \to a_{u_\star}^{(\mathrm{het})}$, $o_u \to o_u^{(\mathrm{het})}$, $o_{u_\star} \to o_{u_\star}^{(\mathrm{het})}$. Eqs. (3.8) and (3.9) give $a_u = a_{u_\star}$ which was obtained before from qualitative considerations. By substituting Eqs. (3.8) and (3.9) into Eq. (3.7) one can find that squeezing in input equals that of environment and output:

$$\frac{i_{u_\star}}{i_u} = \frac{e_{u_\star}}{e_u} = \frac{o_{u_\star}}{o_u}, \tag{3.10}$$

which allows to find optimal input eigenvalues

$$i_u = \frac{1}{2}\sqrt{\frac{e_u}{e_{u_\star}}}, \qquad i_{u_\star} = \frac{1}{2}\sqrt{\frac{e_{u_\star}}{e_u}}. \tag{3.11}$$

For the heterodyne rate one need to replace environment and output eigenvalues in the relations (3.10) and (3.11) by their "heterodyne analogs" (see Eqs. (2.17) and (2.18)). Combining Eq. (3.6) with (3.11) one can obtain optimal c-eigenvalues

$$c_u = N + \frac{1}{2} - i_u + \frac{1-\eta}{\eta}\left(M_{\mathrm{env}} + \frac{1}{2} - e_u\right), \tag{3.12}$$

$$c_{u_\star} = N + \frac{1}{2} - i_{u_\star} + \frac{1-\eta}{\eta}\left(M_{\mathrm{env}} + \frac{1}{2} - e_{u_\star}\right), \tag{3.13}$$

which are the same for both capacity and heterodyne rate except of substitution of different eigenvalues i_u and $i_{u_\star}$.

Finally, the explicit relations for capacity and heterodyne rate in the third stage read

$$\underline{C} = g\left[\eta N + (1-\eta)M_{\mathrm{env}}\right] - g[(1-\eta)N_{\mathrm{env}}], \tag{3.14}$$

$$F^{(\mathrm{het})} = \log_2\left[\eta N + (1-\eta)M_{\mathrm{env}}^{(\mathrm{het})} + \frac{1}{2}\right] - \log_2\left[(1-\eta)N_{\mathrm{env}}^{(\mathrm{het})} + \frac{1}{2}\right]. \tag{3.15}$$

The relation (3.14) generalizes that obtained for LBC with vacuum environment $g(\eta N)$ [11] and, later, with thermal nonsqueezed environment [8]. In turn, Eq. (3.15) generalizes the

relation for heterodyne rate $\log_2(1+\eta N)$ found in [31] for vacuum environment (see also discussion in [11]). Taking into account Eqs. (2.21), (3.14) and (3.15) one can see that the limit (2.22) actually holds, but $\underline{C}^{(0)}$ which is asymptotically logarithmic[3] (3.14) equals Eq. (3.15) after the replacements $M_{\rm env}^{(\rm het)} \to M_{\rm env}$ and $N_{\rm env}^{(\rm het)} \to N_{\rm env}$ (the limits of the ratios $M_{\rm env}^{(\rm het)}/M_{\rm env}$ and $N_{\rm env}^{(\rm het)}/N_{\rm env}$ for $N_{\rm env} \to \infty$ are equal to one).

Previously it was proved that $c_{u_\star} \neq 0$ for the convention chosen ($e_u > e_{u_\star}$), therefore the third stage holds if $c_u > 0$. This is the case if the amount N of input photons is higher than the threshold

$$N_{\rm thr}^{2\to 3} = i_u - \frac{1}{2} - \frac{1-\eta}{\eta}\left(M_{\rm env} - \frac{1}{2} - e_u\right), \tag{3.16}$$

where i_u value should correspond to capacity or heterodyne rate. The threshold $N_{\rm thr}^{2\to 3}$ is nonnegative number which equals zero only for the vacuum environment. As far as the third stage holds only if $N > N_{\rm thr}^{2\to 3}$ and the first stage holds for only $N = 0$, the second stage must correspond to values $0 < N \leqslant N_{\rm thr}^{2\to 3}$. Thus, the type of solution increases its stage in sequence starting from the first stage and ending to the third one if N grows from zero to infinity. This explains the origin of the adopted term "stage" [A5]. Also, it can be interpreted as "the third stage is always the most preferable if energy N is sufficient, otherwise, the second stage should be taken, and the first stage holds if only both the third and the second stage fail to satisfy the constraint". This mnemonic rule is trivial for the single-mode channel, however below its application to multimode channels (memory case) helps to construct optimization algorithms which are not simple to give proof of.

The second stage

Let us move to the case of the second stage. One can show that the Lagrange equations for the capacity and heterodyne rate in this case can be obtained from the system (3.7)-(3.9) by substituting $c_u = 0$ in all equations and removing the derivative with respect to c_u. This is because the variables to find enter in the equations as linear combinations. For the homodyne case the system of equations is the same as for the heterodyne case except of replacements of eigenvalues corresponding to heterodyne.

Then, solving the Lagrange equations for the homodyne rate one can find the ratio

$$\frac{i_{u_\star}}{i_u} = \frac{o_{u_\star}}{a_{u_\star}}, \tag{3.17}$$

which also holds for the heterodyne rate after the replacements $o_{u_\star} \to o_{u_\star}^{(\rm het)}$, $a_{u_\star} \to a_{u_\star}^{(\rm het)}$. For the capacity the Lagrange equations give a *mode transcendent equation* on i_u

$$g_1(\overline{\nu})\left(\frac{1}{o_u} - \frac{1}{a_{u_\star}}\right) - g_1(\nu)\left(\frac{1}{o_u} - \frac{1}{4i_u^2 o_{u_\star}}\right) = 0, \tag{3.18}$$

which results to Eq. (3.17) if g_1-function is taken to zeroth-order approximation (*i.e.* $g_1 \equiv 1$, see Appendix C for the details). Thus, both zeroth-order approximation for capac-

[3]Remember, that according to Eq. (4.24) $g(v) \approx \log_2(v + \frac{1}{2})$.

ity and homodyne rate give the same optimal eigenvalues (see the parallels with Eq. (2.16)):

$$\begin{aligned} & c_u = 0, \\ & c_{u_\star} = 2N + 1 - i_u - \frac{1}{4i_u}, \\ & i_u = \frac{1}{2}\left[\sqrt{1 + (2N+1)\phi + \phi^2/4} - \phi/2\right], \\ & i_{u_\star} = \frac{1}{4i_u}, \\ & \phi = \frac{\eta}{1-\eta} e_{u_\star}^{-1}. \end{aligned} \tag{3.19}$$

Hence, the classical capacity with this approximation is expressible in an explicit form. In turn, the condition $c_{u_\star} > 0$ restricts the admissible region for i_u to the interval

$$N + \frac{1}{2} - \sqrt{N^2 + N} < i_u < N + \frac{1}{2} + \sqrt{N^2 + N}. \tag{3.20}$$

The result for the heterodyne rate is given by the same relations after the replacement $e_{u_\star} \to e_{u_\star}^{(\mathrm{het})}$ in the equation for ϕ.

The first-order approximation for mode transcendent equation (3.18) can be obtained by substituting the approximation (4.25) for g-function. Since Eq. (3.18) cannot be exactly solved within this approximation, it should be solved in the neighbourhood of the zeroth-order solution $i_u^{(0)}$ given by Eq. (3.19) as linear perturbation. Thus, substituting $i_u^{(0)} + \varepsilon_u$ in Eq. (3.18) to i_u and solving for ε_u one can obtain the first-order approximation $i_u^{(1)} = i_u^{(0)} + \varepsilon_u$, where

$$\varepsilon_u = \frac{\eta a_{u_\star} o_u i_u^{(0)} c_{u_\star} (a_{u_\star} - o_u)}{2[\eta^2 (o_u^2 + a_{u_\star}^2 - a_{u_\star} o_u) i_u^{(0)} c_{u_\star} - a_{u_\star}^2 o_u^2 (12\nu^2 + 1)]} \tag{3.21}$$

and all eigenvalues in Eq. (3.21) are calculated through zeroth-order approximation.

Both zeroth-order and first-order approximate optimal eigenvalues found for capacity have to be substituted into exact relation (3.1) instead of its corresponding approximations (e.g. $\log_2(\overline{\nu}/\nu)$ for zeroth-order approximation) used to derive Lagrange equations. Otherwise, the loss in accuracy becomes significant. Although eigenvalues calculated through exact and approximate approaches essentially differ each other, they give rise to almost equal capacities. This can be partially explained by the fact that Holevo χ has zero derivative with respect to eigenvalues in the neighbourhood of solution of Lagrange equations (as they are equations for an optimization problem).

The homodyne rate $\log_2 \sqrt{1 + 4\eta N}$ was found in [31] by supposing both environment and input in vacuum state (see also discussion in [11]). Actually, it can be obtained without solving the optimization problem, by substituting in Eq. (3.3) $i_u = i_{u_\star} = e_u = e_{u_\star} = \frac{1}{2}$ and $c_{u_\star} = 2N$ as it follows from the constraint (3.4). However, since optimal input state is never pure according to Eq. (3.19), that rate holds (approximately) for vacuum environment only if the value of N is close to zero.

Let us demonstrate the above results on the particular case of noiseless channel (η=1). Its capacity equals $C = g(N)$. Its optimal input eigenvalues for the homodyne rate can

be found from Eq. (3.17) by substituting $\eta = 1$, which gives $i_u = N + 1/2$. Its eigenvalues for the heterodyne rate can be obtained from Eqs. (3.11) by taking the limit $\eta \to 1$, which results to $i_u = i_{u_\star} = 1/2$, thus giving $c_u = c_{u_\star} = N$ due to Eq. (3.6) (the second stage cannot be considered for $\eta = 1$ due to threshold $N_{\rm thr}^{2\to 3} = 0$ in this case). Hence, for the noiseless channel it always is [11]

$$F^{(\rm het)} < F^{(\rm hom)} < C, \tag{3.22}$$

where $F^{(\rm hom)} = \log_2(2N + 1)$ [31] and $F^{(\rm het)} = \log_2(N + 1)$, *i.e.* both heterodyne and homodyne rates never achieve the capacity for finite N even for noiseless channel, which keeps the question on optimal decoding still open. In particular, for large values of N inequalities (3.22) read

$$\log_2 N < \log_2 N + 1 < \log_2 N + \frac{1}{\ln 2},$$

i.e. the difference between the rates and the capacity disappears in the limit $N \to \infty$.

3.1.2 Role of channel parameters

In this subsection the dependence of capacity and rates from channel parameters is discussed. The graphs to illustrate the analytical results are given.

Input and environment squeezing

Writing the input covariance matrix in the same form of (2.19), by the replacements $N_{\rm env} \to N_{\rm in}$ and $s \to r$, one can relate the optimal degree of input squeezing $r_{\rm opt}$ to the degree of environment squeezing s. It follows from Eqs. (3.10) and (3.19) that $r_{\rm opt} = s$ for the third stage and

$$r_{\rm opt} \approx r_{\rm opt}^{(0)} = \mathrm{sign}(s) \ln\left[\sqrt{1 + (2N+1)\phi + \phi^2/4} - \phi/2\right] \tag{3.23}$$

for the second stage for capacity to zeroth-order approximation. Analogously, $r_{\rm opt} = s_{\rm het}$ (see Eq. (2.20)) for the heterodyne rate in the third stage. In the second stage both the homodyne and heterodyne rates result to the same relation (3.23), where ϕ depends on $e_{u_\star}^{(\rm het)}$ for the heterodyne case. At the transition point between different stages there is a *kink* in the function $r_{\rm opt}(s)$ (the example with the capacity is shown on Fig.3.1-right). It reflects the fact that different stages correspond to solution of different systems of equations.

The capacity $\underline{C}$ found by the exact and approximate analytical solutions is shown in Fig.3.1-left for fixed N as function of s and for different values of η. The same graph (the case of exact solution) together with rates is shown in Fig.3.5. One can see that in the limit of large s the capacity only depends on the energy constraint N, specifically (see also [A4])

$$\lim_{s\to\infty} \underline{C}(s, \eta, N, N_{\rm env}) = \log_2(2N + 1), \tag{3.24}$$

explaining why all curves $\underline{C}_\eta(s)$ flow together to the same value when $s \to \infty$ (see Fig.3.1-left). This limit also holds for the homodyne rate.

The loci (a_q, a_p) and (o_q, o_p) are plotted in Fig.3.4-left for different values of N and fixed values of $s, \eta, N_{\rm env}$. The resulting curves shows the geometry of the stage transitions and visualize the "quantum water filling" effect for one channel use [9], [14].

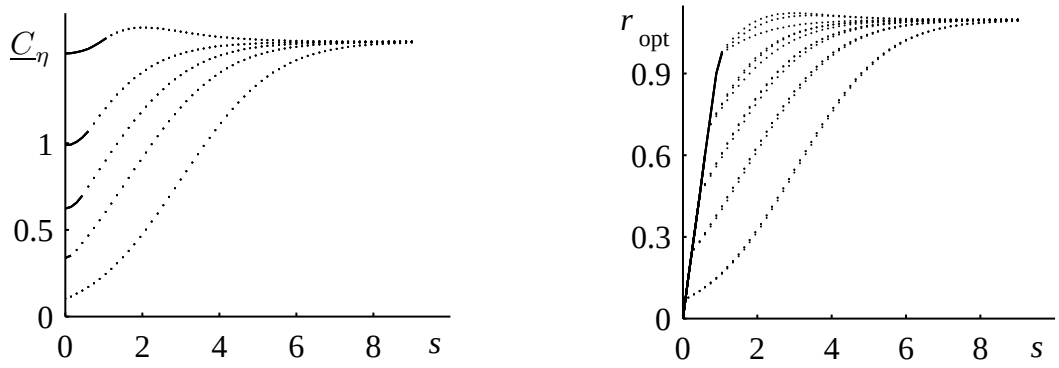

Figure 3.1: Capacity $\underline{C}$ (left) and optimal input squeezing $r_{\rm opt}$ (right) vs s, for values of η going from 0.1 (bottom curve) to 0.9 (top curve) with step 0.2. The values of the other parameters are $N = N_{\rm env} = 1$. On the left, exact and approximate solutions almost coincide. On the right, for each value of η, the zeroth-order approximation, the first-order approximation and the exact solution are plotted (bottom to top). Solid and dotted parts of the curves correspond to the third and second stages, respectively.

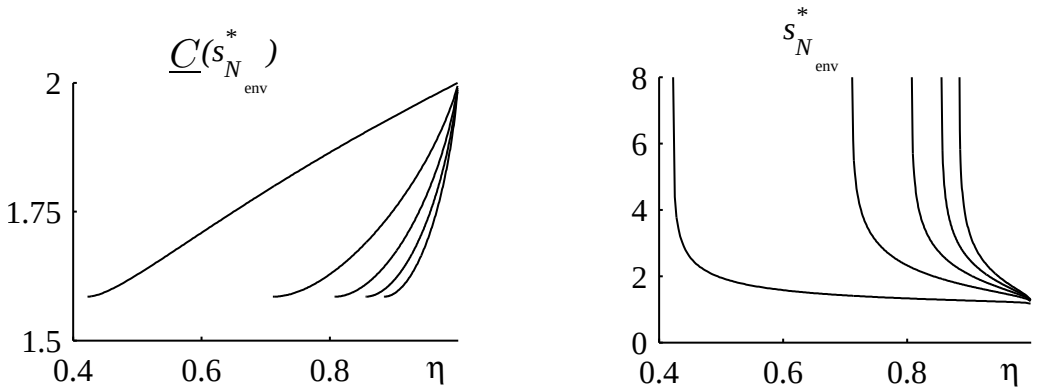

Figure 3.2: Capacity $\underline{C}(s^\star_{N_{\rm env}})$ (left) and optimal environment squeezing $s^\star_{N_{\rm env}}$ (right) vs η for values of $N_{\rm env}$ going from 0 (left curve) to 2 (right curve) with step 0.5. The value of the other parameter is $N = 1$.

Transitional behavior

As it is seen from Fig. 3.1-left, Fig. 3.2-right and Fig. 3.3-right *optimal degree of squeezing in the environment* $s^\star$ (which maximizes the capacity) is finite if transmissivity $\eta > \eta^\star$ and infinite otherwise. The value of $\eta^\star$ will be called *critical transmissivity*. Eigenvalue i_u optimal for $s = s^\star$ can be found from the system of equations $\partial\underline{C}/\partial s = 0$, $\partial\underline{C}/\partial i_u = 0$ taken for the eigenvalues maximizing $\underline{C}$ and belonging to the second stage ($s^\star$ cannot correspond to the third stage as $\partial\underline{C}/\partial s \neq 0$ according to Eq. (3.14)). Taking into account that

$$\frac{d\underline{C}}{ds} = \frac{\partial\underline{C}}{\partial s} + \frac{\partial\underline{C}}{\partial i_u}\frac{\partial i_u}{\partial s},$$

where $\partial\underline{C}/\partial i_u = (\eta/2)\mathcal{F}$ and $\mathcal{F} = 0$ is mode transcendent equation (3.18) one can obtain that $s^\star$ corresponds to $d\underline{C}/ds = \partial\underline{C}/\partial s$ and $i_u = N + 1/2$. The same value of i_u holds in the limit $s \to \infty$, namely, its asymptotic form can be found from the approximation (3.19)

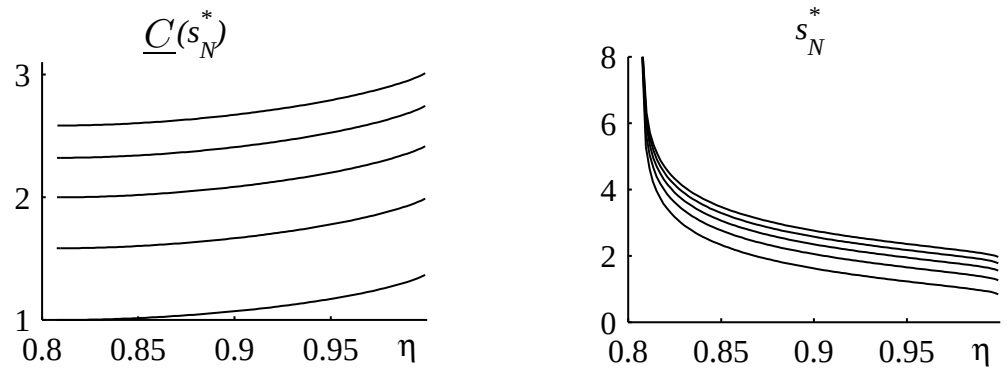

Figure 3.3: Capacity $\underline{C}(s_N^\star)$ (left) and squeezing parameter $s_N^\star$ (right) vs η for values of N going from 0.5 (bottom curve) to 2.5 (top curve) with step 0.5. The value of the other parameter is $N_{\rm env} = 1$.

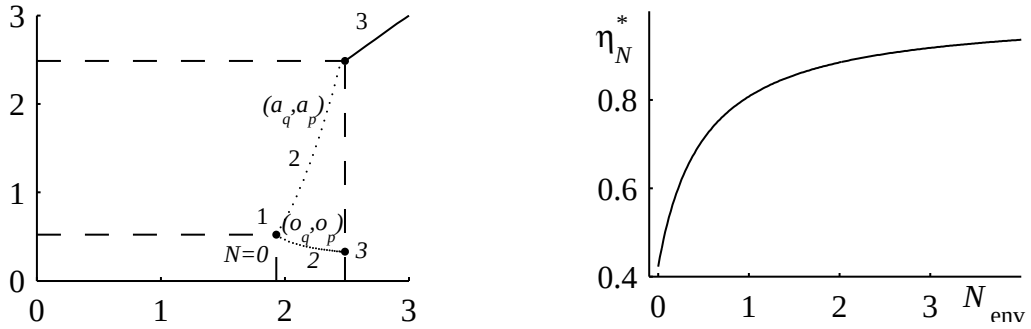

Figure 3.4: On the left, the loci (o_q, o_p) and (a_q, a_p) for different values of N are plotted. The values of other parameters are $N_{\rm env} = s = 1$, $\eta = 0.6$. The second stage is marked by dotted curves. The first stage is a single point at $N = 0$. The whole third stage for the locus (o_q, o_p) is mapped into a single point, as $V_{\rm in}$ does not depend on N in the third stage. On the right, critical transmissivity $\eta^\star$ vs $N_{\rm env}^\star$ is shown.

and equals ($s > 0$)

$$i_u = N + \frac{1}{2} - \frac{4(1-\eta)}{\eta} N(N+1)\left(N_{\rm env} + \frac{1}{2}\right) e^{-s}. \tag{3.25}$$

Substituting Eq. (3.25) into $\partial\underline{C}/\partial s = 0$ taken for the limit $s \to \infty$ and keeping only linear terms over e^{-s} one can get

$$\frac{\partial \underline{C}}{\partial s} = \frac{\left[12^{-1} - (1-\eta)^2\left(N_{\rm env} + \frac{1}{2}\right)^2\right]\left[(2N+1)^{-1} - 2N - 1\right]}{\eta(1-\eta)\left(N_{\rm env} + \frac{1}{2}\right)\ln 2} e^{-s}.$$

As $\partial\underline{C}/\partial s > 0$ and $\partial\underline{C}/\partial s < 0$ give $\eta < \eta^\star$ and $\eta > \eta^\star$, respectively, the *critical parameters* satisfy

$$(1-\eta^\star)\left(N_{\rm env}^\star + \frac{1}{2}\right) = \frac{1}{\sqrt{12}}.$$

The *critical amount of (thermal) photons* $N_{\rm env}^\star$ plays the role similar to critical transmissivity if the family of curves $C(s)$ parametrized by $N_{\rm env}$ for fixed η and N is considered

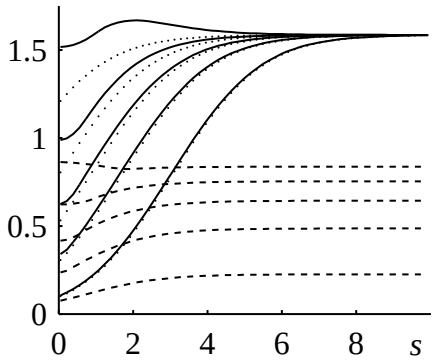

Figure 3.5: Classical capacity $\underline{C}$ (solid curves), heterodyne $F^{(\mathrm{hom})}$ (dashed curves) and homodyne $F^{(\mathrm{het})}$ (dotted curves) rates vs s, for values of η going from 0.1 (bottom curve) to 0.9 (top curve) with step 0.2. The values of the other parameters are $N = N_{\mathrm{env}} = 1$.

instead of the curves from Fig. 3.1-left. In particular, for the vacuum environment

$$\eta^\star = 1 - \frac{1}{\sqrt{3}} \approx 0.42265.$$

The value of $s^\star$ is shown in Fig.3.2-right and Fig.3.3-right as function of η for different values of N_{env} and N respectively. The capacity corresponding to these values of $s^\star$ is plotted in Fig.3.2-left and Fig.3.3-left. The critical transmissivity $\eta^\star$ is drawn in Fig.3.4-right as function of N_{env}.

3.1.3 Concavity of solution

The property of concavity over N for the capacity and rates will be essential below for discussing multi-mode channels, therefore the corresponding derivatives are listed in this subsection.

Let us prove concavity of the function $C(N)$. Formally it is

$$\frac{d\underline{C}}{dN} = \frac{\partial \underline{C}}{\partial N} + \frac{\partial \underline{C}}{\partial i_u}\frac{\partial i_u}{\partial N}.$$

However, as only eigenvalues maximizing $\underline{C}$ are of interest, $\partial\underline{C}/\partial i_u = (\eta/2)\mathcal{F} = 0$ and

$$\frac{d\underline{C}}{dN} = \frac{\partial \underline{C}}{\partial N}.$$

One can show that for all values of N and for both 2nd and 3rd stages

$$\frac{d\underline{C}}{dN} = \frac{\eta}{a_{u_\star}} g_1(\overline{\nu}) > 0. \tag{3.26}$$

The threshold $\mathrm{thr}_{1\to 2}$ is defined as the limit of $d\underline{C}/dN$ for $N \to 0$. It means that u is the quadrature for which $c_u = 0$ after perturbation of N (it is equivalent to the

convention $e_u > e_{u_\star}$). The eigenvalues for input state in this case ($N = 0$) should be taken as corresponding to vacuum state: $i_u = i_{u_\star} = 1/2$. The general relation (3.26) thus gives

$$\mathrm{thr}_{1\to 2} \equiv \frac{d\underline{C}}{dN}(N=0) = \frac{\eta}{o_{u_\star}} g_1(\nu) = \eta \sqrt{\frac{o_u}{o_{u_\star}}} g' \left(\nu - \frac{1}{2}\right). \tag{3.27}$$

Analogously,

$$\mathrm{thr}_{2\to 3} \equiv \frac{d\underline{C}}{dN}(N_{\mathrm{thr}}^{2\to 3}) = \eta\, g_1(\overline{\nu}) = \eta g' \left[\eta \left(i_u - \frac{1}{2}\right) + (1-\eta)\left(e_u - \frac{1}{2}\right)\right], \tag{3.28}$$

where i_u is given by Eq. (3.11).

New **important** comment: it was later found, that for the case of the second stage Eq. (3.29) gives wrong result, since it is only partial (not total) second derivative with respect to N. A correct consideration of the second stage case is given in [A5] and refers to a proof given for additive noise channel in [A6].

The second derivative read

$$\frac{\partial^2 \underline{C}}{\partial N^2} = \begin{cases} \eta^2 (g_2(\overline{\nu}) - g_1(\overline{\nu}))/a_{u_\star}^2 < 0, & \text{for the second stage} \\ \eta^2 g_2(\overline{\nu})/\overline{\nu}^2 < 0, & \text{for the third stage} \end{cases} \tag{3.29}$$

giving the following at the point of *stages transition*:

$$\frac{\partial^2 \underline{C}}{\partial N^2}(N_{\mathrm{thr}}^{2\to 3} - 0) = \frac{\partial^2 \underline{C}}{\partial N^2}(N_{\mathrm{thr}}^{2\to 3} + 0) - \frac{\eta^2}{\overline{\nu}^2} g_1(\overline{\nu}).$$

Because it always is $g_2 < 0$, $g_1 > 0$, the convexity is preserved on the whole region of $N \in [0, \infty)$:

$$\frac{\partial^2 \underline{C}}{\partial N^2}(N_{\mathrm{thr}}^{2\to 3} - 0) < \frac{\partial^2 \underline{C}}{\partial N^2}(N_{\mathrm{thr}}^{2\to 3} + 0),$$

while the first derivative is continuous in this point. Notice, that

$$\max_N \frac{\partial \underline{C}}{\partial N} = \frac{\partial \underline{C}}{\partial N}(N=0) \leqslant \infty, \tag{3.30}$$

where equality is achieved only by pure environment state $e_u = e_{u_\star} = 1/2$.

Thus, single-mode capacity for fixed values of $e_u, e_{u_\star}$ and η can be considered as the concave function:

$$N \longrightarrow \boxed{\underline{C} = \underline{C}(N)} \longrightarrow \underline{C}, \tag{3.31}$$

i.e. some "blackbox" returning the value of $\underline{C}$ given N "at input". The derivatives for the rates can be obtained by doing the replacement $g_1 \to 1/\ln 2$, $g_2 \to -1/\ln 2$ in Eqs. (3.26) and (3.29). Except of this replacement, for the heterodyne rate $\overline{\nu}$ and $a_{u_\star}$ should be taken in "heterodyne form". Hence, both heterodyne and homodyne rates are also concave functions which can be treated in the same "blackbox" form.

3.2 Multi-mode channel: memory case

Let us move to the case of the single use of multi-mode LBC. Its capacity and rates are the same as for n uses of the corresponding single-mode memory channel.

3.2.1 Convex separable programming

The optimization problem for multi-mode channel is formulated as follows. One needs to find the maximum over the variables i_{uk}, c_{uk}, and $c_{u_\star k}$ for the following functions:

$$\underline{C}_n = \frac{1}{n}\sum_{k=1}^{n}\left[g\left(\overline{\nu}_k - \frac{1}{2}\right) - g\left(\nu_k - \frac{1}{2}\right)\right], \tag{3.32}$$

$$F_n^{(\mathrm{het})} = \frac{1}{n}\sum_{k=1}^{n}\left[\log_2 \overline{\nu}_k^{(\mathrm{het})} - \log_2 \nu_k^{(\mathrm{het})}\right], \tag{3.33}$$

$$F_n^{(\mathrm{hom})} = \frac{1}{2n}\sum_{k=1}^{n}\left[\log_2 a_{u_\star k} - \log_2 o_{u_\star k}\right] \tag{3.34}$$

with the constraints

$$\begin{aligned} &i_{uk} > 0, \\ &c_{uk}, c_{u_\star k} \geqslant 0, \\ &\frac{1}{n}\sum_{k=1}^{n}\left[i_{uk} + \frac{1}{4i_{uk}} + c_{uk} + c_{u_\star k}\right] = 2N + 1. \end{aligned} \tag{3.35}$$

The problem for capacity[4] can be reformulated as finding the maximum for sum of concave[5] functions (each of them depends on one varibale)

$$\underline{C}_n(N) = \sum_{k=1}^{n} X_k(N_k) = \frac{1}{n}\sum_{k=1}^{n} C_k \tag{3.36}$$

over the distribution $P(N_k)$ of positive numbers N_k satisfying the constraint

$$N = \sum_{k=1}^{n} N_k, \qquad N_k = \frac{1}{2n}\left[i_{uk} + \frac{1}{4i_{uk}} + c_{uk} + c_{u_\star k} - 1\right] \geqslant 0, \tag{3.37}$$

where N_k is the amount of energy granted for kth mode, $X_k = C_k/n$ and $C_k = C_k(i_{uk}, c_{uk}, c_{u_\star k})$ (see the definition (2.14)) is parametrized by fixed parameters e_{uk}, $e_{u_\star k}$ and η, *i.e.* C_k depends on the only eigenvalues belonging to kth mode. Thus, the total optimization problem is splitted in two tasks: the first task is "internal optimization" inside each mode (see "box" (3.31)) and the second task is "external optimization" which finds the optimal distribution $P(N_k)$ of the total energy N over "boxes" to get optimal output sum $\sum_{k=1}^{n} X_k$:

$$\begin{aligned} N_1 &\longrightarrow \boxed{X_1 = X_1(N_1)} \longrightarrow X_1 \\ &\cdots\cdots\cdots\cdots\cdots \\ N_n &\longrightarrow \boxed{X_n = X_n(N_n)} \longrightarrow X_n \end{aligned}$$

This "external optimization" problem is known in mathematics as *convex separable programming* which was solved in [32], [33]. In particular, the following theorem based on

[4]The case of rates is completely analogous to capacity, therefore here it is omitted.

[5]The concavity of single-mode C_k over its energy constraint N_k was proved in previous section.

concavity of target function was proved [32]:

> Theorem: A feasible solution $\{N_k\}$ is an optimal solution to problem (3.36), (3.37) if and only if there exists a $\lambda \in \mathbb{R}$ such that
>
> $$N_k = 0, \qquad \text{if} \quad \lambda \geqslant \frac{\partial X_k}{\partial N_K}(N_k = 0)$$
>
> $$N_k : \lambda = \frac{\partial X_k}{\partial N_K}(N_k), \qquad \text{if} \quad \lambda < \frac{\partial X_k}{\partial N_K}(N_k = 0)$$

Thus, this theorem states that any solution of "external optimization" problem satisfying its Lagrange equations is optimal because it is unique. Taking into account (3.30) one can see that $\lambda \in (0, \lambda_{\max})$ for $N > 0$, where

$$\lambda_{\max} = \max_k \frac{\partial X_k}{\partial N_k}(N_k = 0).$$

In the following the notion of *stage* will be used which is defined for each mode in complete analogy with the single-mode case. It allows the optimization problem to be interpreted as the search for the optimal *modes distribution over stages*. In particular, the case $N_k = 0$ holds if and only if kth mode belongs to the first stage, and the case $\lambda = \lambda_{\max}$ corresponds to zero capacity, where all modes are in the first stage. Analogously, if it is

$$\lambda < \min_k \frac{\partial X_k}{\partial N_k}(N_k = 0)$$

only the second and the third stages exist (by comparing N_k granted for kth mode with its threshold value $N_{\text{thr}}^{2\to3}$ (see Eq. (3.16)) one can obtain its actual stage).

The following algorithm to solve "external optimization" problem can be proposed. Let us choose any $\lambda^\star$ from the interval $(0, \lambda_{\max})$. Then, the contribution N_k of kth mode can be found by solving the equation

$$\lambda^\star = \frac{\partial X_k}{\partial N_k}(N_k),$$

if

$$\lambda^\star < \frac{\partial X_k}{\partial N_k}(N_k = 0).$$

Otherwise, $N_k = 0$ has to be chosen. After finding N_k values for all $k = 1, \ldots n$, the sum $\sum_{k=1}^n N_k$ should be compared with N. If $N < \sum_{k=1}^n N_k$, the value $\lambda = \lambda^\star/2$ should be chosen for the next iteration, otherwise $\lambda = (\lambda_{\max} - \lambda^\star)/2$ should be taken (thus, the Lagrange equations can be considered as giving feasible solution for *any* λ, the only difference is that such the solution corresponds to another value of N). The above iteration should be repeated again for new λ chosen. By repeating such iterations sufficient times the value λ corresponding approximately to actual N can be found. In other words, Lagrange equations can be interpreted as the single transcendent equation on λ which can be solved, e.g. by the above method of bisection.

As far as the solution is unique it is sufficient to prove convergence of the algorithm suggested to find modes distribution over stages, which can be done as follows. Notice, that λ and N are related each other by one-to-one correspondence, and the dependence

$\lambda(N)$ is monotonic. In particular, the limit $\lambda \to 0$ corresponds to the limit $N \to \infty$, and the value $\lambda = \lambda_{\max}$ corresponds to $N = 0$. Thus, as far as the only unique λ corresponds to N given, solving the system of Lagrange equations as the single transcendent equation on variable $\lambda \in (0, \lambda_{\max}]$ one see that the algorithm always converges to the solution.

3.2.2 Classical capacity and rates

The method to find classical capacity and rates discussed below is completely equivalent to the general scheme presented in the previous section and results to the same system of equations to solve. However, it mainly operates with eigenvalues i_{uk}, c_{uk} and $c_{u_\star k}$ as variables instead of N_k, which allows to develop another "representation" of the solution and optimization algorithms.

To simplify the calculations here will be applied a technique similar to the simplex method in optimization theory. Assuming monotonic dependence on N of the eigenvalues $\{c_{uk}\}$ maximizing $\underline{C}_n$ (which is supported by numerical investigation), their sign will not be specified in Lagrange equations. At first, let us consider the formal solution of Lagrange equations assuming negative eigenvalues as result, then it will be shown how to eliminate them.

The Lagrange function for the capacity of n-modes channel reads

$$L = \frac{\chi_n}{n} - \lambda \left(\frac{1}{n} \sum_{k=1}^{n} [i_{qk} + i_{pk} + \ c_{qk} + c_{pk}] - 2N - 1 \right).$$

When all modes belong to the third stage, the eigenvalues of $\overline{V}_{\text{out}}$ are all equal and the solution reads

$$c_{uk} = N + \frac{1}{2} - i_{uk} + \frac{1-\eta}{\eta} \left(M_{\text{env}} + \frac{1}{2} - e_{uk} \right), \tag{3.38}$$

$$i_{uk} = \frac{1}{2} \sqrt{\frac{e_{uk}}{e_{u_\star k}}}, \tag{3.39}$$

giving

$$\underline{C}_n = g[\eta N + (1-\eta) M_{\text{env}}] - \frac{1}{n} \sum_{k=1}^{n} g\left[(1-\eta) N_{\text{env}}^{(k)}\right], \tag{3.40}$$

where $N_{\text{env}}^{(k)} = \sqrt{e_{qk} e_{pk}} - 1/2$. For the case of heterodyne rate Eq. (3.38) is the same, but i_{uk} is given by the relation (3.39) after the replacements $e_{uk} \to e_{uk}^{(\text{het})}$, $e_{u_\star k} \to e_{u_\star k}^{(\text{het})}$. Hence, the heterodyne rate results to

$$F^{(\text{het})} = \log_2 \left[\eta N + (1-\eta) M_{\text{env}}^{(\text{het})} + \frac{1}{2} \right] - \frac{1}{n} \sum_{k=1}^{n} \log_2 \left[(1-\eta) N_{\text{env}}^{(k)(\text{het})} + \frac{1}{2} \right],$$

where $N_{\text{env}}^{(k)(\text{het})}$ is $N_{\text{env}}^{(\text{het})}$ (see Eq. (2.20)) calculated for kth mode.

Let us now move to the general case. At first, it will be assumed that the correct distribution of modes over stages is already found. Then, suppose to know that the eigenvalue

$a_{u_\star h}$ (for the mode h) for capacity belongs to the second stage and $c_{uh} = 0$, it follows the transcendent equation for i_{uh}

$$g_1(\overline{\nu}_h)\left(\frac{1}{o_{uh}} - \frac{1}{a_{u_\star h}}\right) - g_1(\nu_h)\left(\frac{1}{o_{uh}} - \frac{i_{u_\star h}}{i_{uh}o_{u_\star h}}\right) = 0, \tag{3.41}$$

where

$$c_{u_\star h} = \frac{a_{u_\star h} - (1-\eta)\, e_{u_\star h}}{\eta} - \frac{1}{4i_{uh}},$$
$$i_{u_\star h} = \frac{1}{4i_{uh}}.$$

This equation has real roots if both $\overline{\nu}_h, \nu_h > 1/2$, giving

$$i_{uh} > \max\left\{\frac{1}{\eta}\left(\frac{1}{4a_{u_\star h}} - (1-\eta)e_{uh}\right), 0\right\}. \tag{3.42}$$

In turn, the requirement $\overline{\nu}_h > \nu_h$ leads to the inequality

$$i_{uh} > \frac{\eta}{4(a_{u_\star h} - (1-\eta)e_{u_\star h})}. \tag{3.43}$$

Depending on the value of $a_{u_\star h}$, equation (3.41) can admit one root satisfying (3.43) or none.

Equation (3.41) can be formally written as the dependence $a_{u_\star h} = f_h(i_{uh})$. Taking into account that λ is the only parameter linking the Lagrange-equations of different modes, and considering zeroth-order approximation for g_1-function, one can define a new variable x

$$x := a_{qm} = a_{pm} = a_{ql} = a_{pl} = a_{qh} = f_h(i_{ph}) = a_{pt} = f_t(i_{qt}), \tag{3.44}$$

getting a chain of equalities relating *all* modes of the second and third stages. The exact form of the above chain which does not use approximations reads (see Eq. (3.26))

$$\frac{g_1(\overline{\nu}_m)}{a_{qm}} = \frac{g_1(\overline{\nu}_m)}{a_{pm}} = \frac{g_1(\overline{\nu}_l)}{a_{ql}} = \frac{g_1(\overline{\nu}_l)}{a_{pl}} = \frac{g_1(\overline{\nu}_h)}{a_{qh}} = \frac{g_1(\overline{\nu}_t)}{a_{pt}}.$$

Here modes m and l belong to the third stage, while modes h and t to the second stage ($c_{ph} = c_{qt} = 0$). Modes of the first stage are not included in (3.44) and they all give V_{in}-eigenvalues equal to $1/2$. If some mode belongs to the third stage, its V_{in}-eigenvalues can be found from the relation (3.39). Below in this chapter only the case of approximation (3.44) will be considered, because the general solution does not allow to essentially simplify the relations.

Taking into account stages discrimination, equation (2.3) can be rewritten as

$$\sum_{\{2,3|c_{uk}\neq 0\}} \left[\eta\overline{i}_{uk} + (1-\eta)e_{uk}\right] = [2n_3 + n_2]x, \tag{3.45}$$

where $\overline{i}_{uk}$ are eigenvalues of $\overline{V}_{\text{in}} := V_{\text{in}} + V_{\text{cl}}$. Furthermore, n_j is the number of modes belonging to j-th stage ($j = 1, 2, 3;\ n = n_1 + n_2 + n_3$) and $\sum_{\{2,3|c_{uk}\neq 0\}}$ stands for the

summation over all eigenvalues of second and third stages, except for the uk-th ones corresponding to $c_{uk} = 0$. Also, the energy constraint (1.24) can be rewritten as

$$\sum_{\{2,3|c_{uk}\neq 0\}} \bar{i}_{uk} = 2n\left[N + \frac{1}{2}\right] - n_1 - \sum_{k}{}'' i_{uk}, \tag{3.46}$$

where $i_{uk} = f_k^{-1}(x)$ and the double prime sum extends over uk-th eigenvalues of the second stage, such that $c_{uk} = 0$. Substituting Eq. (3.46) into Eq. (3.45) one can get a transcendent equation for the single variable x. Since all unknown eigenvalues can be expressed through x (see Eqs. (3.44)) one can formally arrive at $\underline{C}_n$.

To the zeroth-order approximation (4.24) the relation $i_{uk} = f_k^{-1}(x)$ (see Eq. (3.41)) gives

$$i_{uk} \approx i_{uk}^{(0)} = \frac{1}{8}\left[\sqrt{\phi_k^2 + 16x\phi_k/\eta} - \phi_k\right], \tag{3.47}$$

where ϕ_k equals ϕ defined by Eq. (3.19) after the replacement $e_{u_\star} \to e_{u_\star k}$. The approximation (3.47) allows to express $\underline{C}_n$ as function of solution of only one algebraic equation for one variable x. By considering the term $1/v^2$ of the decomposition (4.23) in Eq. (3.41), one can obtain the first-order approximation for the relation $i_{uk} = f_k^{-1}(x)$. Since Eq. (3.41) cannot be exactly solved within this approximation, it should be solved in neighbourhood of the zeroth-order solution as linear perturbation. Thus, substituting $i_{uk}^{(0)} + \varepsilon_{uk}$ in Eq. (3.41) instead of i_{uk} and solving for ε_{uk} one can find the first-order approximation $i_{uk}^{(1)} = i_{uk}^{(0)} + \varepsilon_{uk}$, where

$$\varepsilon_{uk} = \frac{(x - o_{uk})(x - o_{u_\star k})o_{uk}i_{uk}^{(0)}}{[2(o_{uk}^2 + x^2 - (o_{uk} + o_{u_\star k})x) + (12o_{uk}^2 + 1)\nu_k^2]i_{uk}^{(0)}\eta - 2(1 + 12\nu_k^2)o_{uk}^2 x} \tag{3.48}$$

and all eigenvalues in Eq. (3.48) are calculated to zeroth-order approximation.

Notice that the first-order approximation considered for the case of single-mode channel does not coincide with $i_u^{(1)}$ found. Actually, one needs to jointly solve two equations in the case of general method applied to one channel use: the transcendent equation (3.41) and the equation for x (see Eqs. (3.45) and (3.46)), where only Eq. (3.41) is approximated. However, the equation for x becomes analytically solvable in the case of one channel use, allowing us to reduce the original two equations to a single one given by (3.18).

For the case of rates the chain (3.44) and the equations (3.45), (3.46) are the exact relations except of absence of the third stage for the homodyne rate ($n_3 = 0$). Eq. (3.47) holds also for the rates except of ϕ_k which has to be calculated using $e_{u_\star k}^{(\mathrm{het})}$ instead of $e_{u_\star k}$ for the heterodyne case.

Finally, let us discuss on how to find the correct distribution of modes over the stages. As far as Lagrange-conditions themselves do not provide effective method to find stages distribution, one needs to use some *a proiri* properties to write an effective algorithm. Since it was conjectured (supported by numerics) that c_{uk}-eigenvalues are monotonic functions of N, the optimum for each mode has to be the third stage, or the second if the third is not admissible, or even the first if also the second one is not admissible. The third stage implies the existence of a solution inside some volume, the second stage — a solution on the surface of that volume, while the first stage — a solution on the edges of that surface. If the value of N is large enough, the solution is always inside a volume, so that all modes

are in the third stage. By decreasing the value of N, the eigenvalues c_{uk} pass from the volume to the wall, and then to the edges. On the basis of these arguments one can develop two algorithms: *static* and *dynamic*.

The first step for both algorithms is the same: the positivity of all c_{uk} that were found is checked through the relations (3.38). If all of them are positive, $\underline{C}$ is given by the explicit analytical relation (3.40) and the problem is already solved. If this is not the case, one has to move on to the next steps.

- The static algorithm gives the following continuation on the bases of c_{uk}-signs found in the first step. One should ascribe the third stage to modes with all positive c_{uk}-eigenvalues, the second stage to modes with only one negative eigenvalue c_{uk} and the first stage to modes with both negative c_{uk}. All negative c_{uk} should be marked as already found and equal to zero. According to this distribution the set of Lagrange-equations should be formally solved (once again). If some second stage modes do not have a solution according to Eq. (3.41) they have to be marked as belonging to the first stage. Here the condition (3.43) is neglected for the second stage modes, as violation of it implies negative c_{uk}, thus their stage will be changed to the first one by the algorithm itself. If all found c_{uk} are finally non-negative the problem is solved. If it is not, the procedure is iterated up until all c_{uk} will become non-negative. This algorithm can be then considered as a consecutive correction of stages distribution.

- The dynamic algorithm continues after the first step as follows. One should solve the transcendent equation on x by choosing different stages distributions for different values of x (during iterations). In particular, each mode at beginning is calculated as belonging to the third stage for the current value of x. If this leads to negative c_{uk}, the mode is marked as belonging to the second or the first stage in analogy with the static algorithm (if some second stage modes violate Eq. (3.43) their stage should be marked as the first one). Thus, the stages distribution is made admissible, in quantum sense, for every value of x. The distribution of stages corresponding to a root of the equation for x is considered to be valid and can be used to calculate the correct eigenvalues.

Both static and dynamic algorithms always yield the same stages distribution. The difference between the two algorithms can be clarified as follows. There are two effective unknown "variables" for Lagrange-equations: stages distribution and x. One of these variables has to be set as internal and the another one as external during maximization of χ_n. The static algorithm uses x as internal variable, while the dynamic algorithm uses stages distribution for that. Since dynamic algorithm is usually faster, below only it will be used. Also notice that the eigenvalues i_{uk} are always obtained as positive through these algorithms, therefore their positivity is not specified in Lagrange equations.

If number of channel uses tends to infinity the discussed procedure can be properly generalized by changing the transcendent equations to equations on functions (spectral densities). However, if the considered model has some simple symmetries over stages, the general solution can be simplified by considering some parameters which mark the boundaries of stages. In the next chapter an example along this line will be shown.

Chapter 4

A model for memory effects

In this chapter a particular model of channel environment is considered, which allows to test the general solution given in the previous chapter. To introduce the memory effect among different channel uses, the environment modes are supposed to be initially in a correlated state, actually a multimode squeezed thermal state. Multimode squeezed states depending on two parameters are considered as introduced in [34], so that the covariance matrix V_{env} is chosen as

$$V_{\text{env}} = \left(N_{\text{env}} + \frac{1}{2}\right) \begin{bmatrix} \exp(s\Omega) & 0 \\ 0 & \exp(-s\Omega) \end{bmatrix}, \tag{4.1}$$

where N_{env} is the average number of thermal photons per mode in the environment and $s \in \mathbb{R}$ represents the memory strength (for $s = 0$ the memoryless case is recovered). Here, the $n \times n$ matrix Ω is taken to be

$$\Omega = \begin{pmatrix} 0 & 1 & \cdots & \cdots & 0 \\ 1 & 0 & 1 & \cdots & 0 \\ \vdots & 1 & 0 & 1 & \cdots & 0 \\ \vdots & \vdots & \ddots & \ddots & \ddots & \\ \vdots & \vdots & & \ddots & \ddots & 1 \\ 0 & 0 & \cdots & 1 & 0 \end{pmatrix}. \tag{4.2}$$

Notice that the memory effect is symmetric among all modes and decays over the number of uses. Actually, if the set of V_{env} matrix elements belonging to a fixed row is considered as a discrete function, this is well fitted by a Gaussian having width $2\sqrt{|s|}$. Such exponential decay of correlations makes the noise in the channel non-Markovian and the channel not strictly forgetful [35].

4.1 Approximate solution

In this section the approximate solution based on the chain (3.44) is considered, and only asymptotic behavior of the channel is discussed. That implies to take the limit $n \to \infty$ in the equations of previous chapter. It can be treated for some relations as the limit of Riemann sums resulting to the integral expressions. Instead of a set of equations on

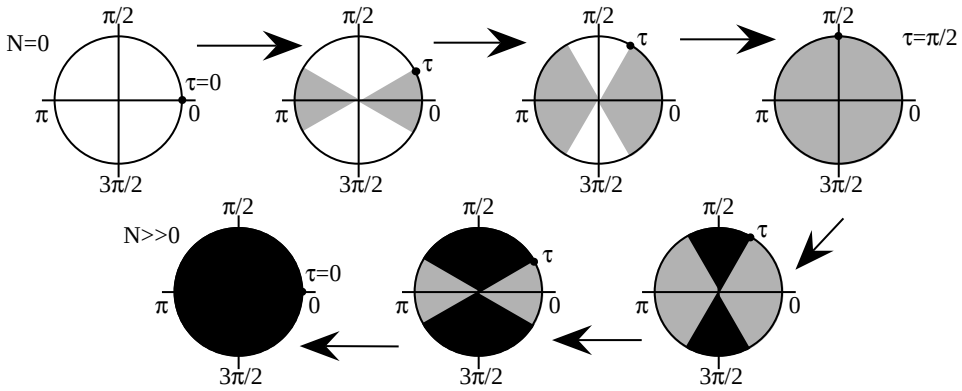

Figure 4.1: Schematic representation of the "quantum water filling" for the model $\Omega_{ij} = \delta_{i,j+1} + \delta_{i,j-1}$. The angle ξ parametrizing the spectral density corresponds to polar angle. White, grey and black sectors correspond to the first, second and third stages, respectively. Arrows show change of stages with increasing of N. The parameter τ marks the points of stages transition.

eigenvalues one can get a set of equations on functions which are spectral densities for the involved (infinite-dimensional) matrices. Below the spectral densities will be denoted by the same symbols as proper eigenvalues, but written in calligraphic with the mode number h replaced by a continuous parameter ξ, *i.e.*, $i_{uh} \to \mathcal{I}_{u\xi}$, $o_{qh} \to \mathcal{O}_{q\xi}$, etc.

Suppose that all modes belong to the third stage, which holds true if (see Eq. (3.38))

$$w := \frac{1}{2|s|} \ln \frac{\eta\,(2N+1) + (1-\eta)(2N_{\rm env}+1)\,I_0(2s)}{\eta + (1-\eta)(2N_{\rm env}+1)} \geq 1, \tag{4.3}$$

where I_0 is the modified Bessel function of the first kind and zero-order. The lower bound $\underline{C}$ in this case is given by Eq. (3.14), where $M_{\rm env}$ should be replaced by

$$M_{\rm env} = \left(N_{\rm env} + \frac{1}{2}\right) I_0(2s) - \frac{1}{2}.$$

This example explicitly shows the possibility of an enhancment of the lower bound on the classical capacity with increasing degree of memory s.

It is convenient to use the parameter ξ as arising from the spectrum of $V_{\rm env}$-matrix (see Eq. (4.13))

$$\mathcal{E}_{u\xi} = \left(N_{\rm env} + \frac{1}{2}\right) e^{\pm 2s\cos\xi}, \tag{4.4}$$

labeling both modes (if $\xi \in [0,\pi]$) and eigenvalues (if $\xi \in [0,2\pi]$). Plus and minus in Eq. (4.4) stand for $u = q$ and $u = p$, respectively. Due to the mirror symmetry of eigenvalues (4.4) over quadratures, the symplectic spectrum and the stages distribution have to be symmetric with respect to the point $\pi/2$, therefore the spectral densities below are considered only in the interval $[0,\pi/2]$.

If $w < 1$ it is possible to have one of the following stages distributions according to the properties of the derivative $\partial\underline{C}_\xi/\partial N_\xi(N_\xi = 0)$ studied in zeroth-order approximation[1] (accordingly to the procedure of the previous chapter):

[1]Quite generally, without any approximation this distribution of modes over stages does not hold.

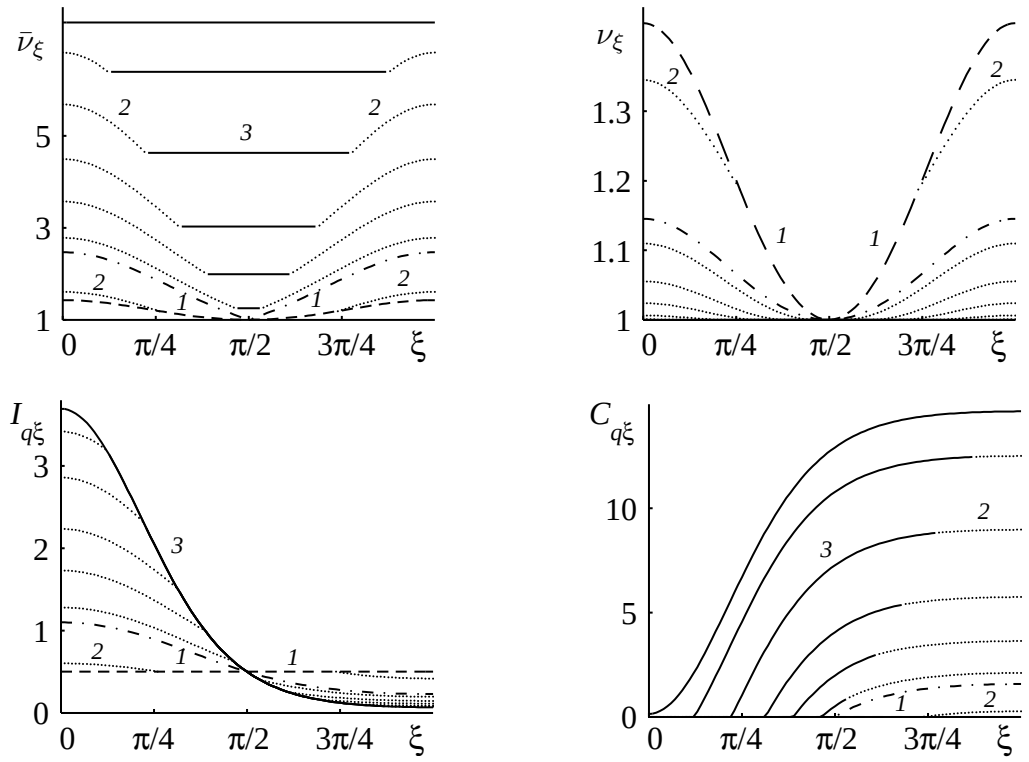

Figure 4.2: Going from top-left clockwise the spectral densities $\bar{\nu}_\xi, \nu_\xi, \mathcal{C}_{q\xi}, \mathcal{I}_{q\xi}$ (for $\Omega_{ij} = \delta_{i,j+1} + \delta_{i,j-1}$) are plotted vs the parameter ξ for $N = 0, 0.05, 0.67, 1, 2, 3.5, 6, 9, 11$ (from bottom to top curve for quantities $\bar{\nu}_\xi, \mathcal{C}_{q\xi}, \mathcal{I}_{q\xi}$, and from top to bottom curve for quantity ν_ξ). Solid, dotted and dashed parts of curves correspond to *(3,3,3)*, *(2,3,2)* and *(2,1,2)* cases, respectively. Dash-dotted curve corresponds to the case of all modes belonging to the second stage. The values of other parameters used are $N_{\rm env} = s = 1$, $\eta = 0.5$.

i) a mixture of second and third stages *(2,3,2)*;

ii) a mixture of second and first stages *(2,1,2)*;

iii) all modes belonging to the second stage *(2,2,2)* which happens for a single value N_2 of the parameter N, given s, η and $N_{\rm env}$.

If $N > N_2$ or $N < N_2$ the case *(2,3,2)* or *(2,1,2)* holds with the center of the interval $[0, \pi]$ filled by the third or the first stage, respectively. The point of stages transition will be labelled by $\tau \in [0, \pi/2]$. The possible stages distributions and dependence of τ from N are sketched in Fig.4.1. The continuity of the spectral density $\mathcal{C}_{u\xi}$ at points of stages transition τ requires to hold $\mathcal{A}_{u\tau} = \mathcal{O}_{u\tau}$ which can be rewritten as

$$x = x(\tau) = \eta \mathcal{I}_{u\tau} + (1 - \eta)\mathcal{E}_{u\tau}. \tag{4.5}$$

Here $u = q$ gives $\mathcal{I}_{q\tau} = e^{2s\cos\tau}/2$ (see Eq. (3.38)) for *(2,3,2)* and $u = p$ gives $\mathcal{I}_{p\tau} = 1/2$ for *(2,1,2)* (different quadratures are used in these cases because of either $\mathcal{C}_{q\xi}$ or $\mathcal{C}_{p\xi}$ has a transition point belonging to the interval of τ).

Then, the transcendent equation for x (see Eqs. (3.45) and (3.46)) can be rewritten as an equation for τ

$$\eta \left[N + \frac{\tau_1}{\pi} - \frac{1}{\pi} \int_0^\tau \mathcal{I}_{q\xi}\, d\xi \right] + \frac{1 - \eta}{\pi} \int_0^{\tau_2} \mathcal{E}_{p\xi} d\xi = \frac{\tau_2}{\pi} x, \tag{4.6}$$

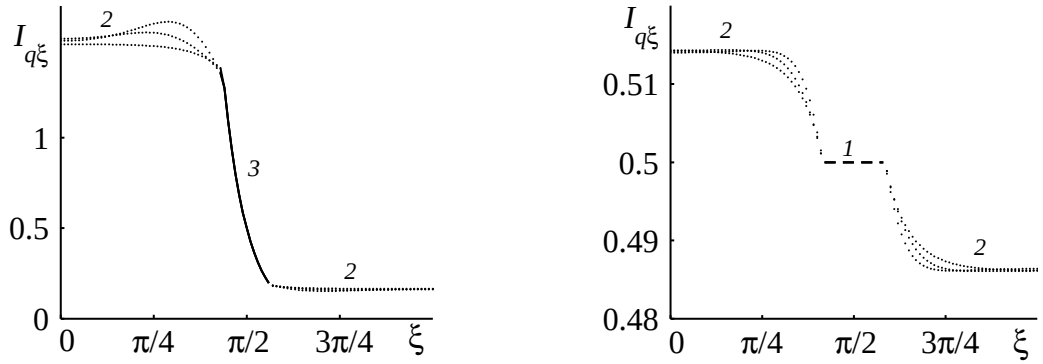

Figure 4.3: Exact solution, first-order and zeroth-order approximations for spectral density $\mathcal{I}_{q\xi}$ vs ξ for $N = 1$ (left) and $N = 0.01$ (right). The values of other parameters are $N_{\rm env} = 0.5$, $s = 2.5$, $\eta = 0.95$. Solid, dotted and dashed parts of curves correspond to *(3,3,3)*, *(2,3,2)* and *(2,1,2)* cases, respectively. Functions with maximum and minimum variations correspond to exact solution and zeroth-order approximation, respectively.

where (τ_1, τ_2) is equal to (τ, τ) for *(2,1,2)* and to $(\pi/2, \pi - \tau)$ for *(2,3,2)*. Moreover, x is given by Eq. (4.5) and $\mathcal{I}_{q\xi}$ is the spectral density for the second stage which can be found as solution of functional equation obtained from Eq. (3.41) or its approximations (see Eqs. (3.47), (3.48)) after the replacements discussed at the begining of this section. By substituting $\tau = \pi/2$ in Eq. (4.6) one can find N_2. Comparing it with the actual energy restriction one can get correct stages distribution. Then, solving Eq. (4.6) with the found stages distribution one can arrive at τ and x. Finally, $\underline{C}$ is expressed through these parameters as follows (see Eqs. (1.27) and (1.28)):

$$\underline{C} = \left(1 - \frac{2}{\pi}\tau_3\right)\left[g\left(x - \frac{1}{2}\right) - g((1-\eta)N_{\rm env})\right] + \frac{2}{\pi}\int_0^{\tau}\left[g\left(\sqrt{x\mathcal{O}_{q\xi}} - \frac{1}{2}\right) - g\left(\sqrt{\mathcal{O}_{q\xi}\mathcal{O}_{p\xi}} - \frac{1}{2}\right)\right]d\xi,$$

where

$$\mathcal{O}_{q\xi} = \eta\mathcal{I}_{q\xi} + (1-\eta)\mathcal{E}_{q\xi}, \tag{4.7}$$

$$\mathcal{O}_{p\xi} = \frac{\eta}{4}\mathcal{I}_{q\xi}^{-1} + (1-\eta)\mathcal{E}_{p\xi}, \tag{4.8}$$

τ_3 is equal to $\pi/2$ for *(2,1,2)* and to τ for *(2,3,2)*.

The "quantum water filling" effect for the considered model is shown in Fig.4.2 for symplectic spectral densities $\overline{\nu}_\xi$, ν_ξ and spectral densities $\mathcal{C}_{q\xi}$, $\mathcal{I}_{q\xi}$. Graphs of $\mathcal{I}_{q\xi}$ calculated through exact solution[2], zeroth-order and first-order approximations are shown in Fig.4.3. Despite some visible difference between exact and approximate spectral densities the corresponding symplectic spectral densities are almost equal, thus resulting to a difference less than 0.05% between $\underline{C}$ calculated exactly and approximately. The small value of this difference can be explained analogously to the single-mode case discussed in the previous chapter.

[2]In this section the term "exact solution" means that mode transcendent equation is not approximated,

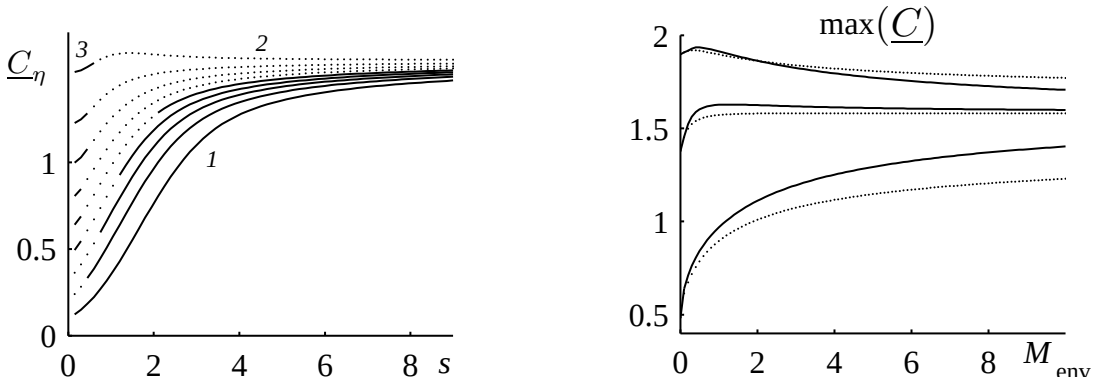

Figure 4.4: On the left, the quantity $\underline{C}$ is plotted vs s for values of η going from 0.1 (bottom curve) to 0.9 (top curve) with step 0.1. The values of the other parameters are $N = N_{\rm env} = 1$. Solid parts of curves correspond to the *(3,3,3)* and *(2,1,2)* cases, respectively. Dotted part of curves correspond to *(2,3,2)* case. On the right, the maximum of $\underline{C}$ over $V_{\rm env}$ is plotted vs $M_{\rm env}$ for values of $\eta = 0.1, 0.5, 0.9$ going from bottom to top curve. Solid and dotted curves corresponds to $\Omega = I$ and $\Omega_{ij} = \delta_{i,j+1} + \delta_{i,j-1}$, respectively. The value of the other parameter is $N = 1$.

The solution of Lagrange equations can be interpreted as "quantum water filling" in analogy with usual (classical) "water filling" introduced for classical Gaussian channels with memory (see e.g. [14]). The dependence of the found spectral densities (also symplectic ones) from N is similar to filling a vessel with water. The form of the vessel is defined by the model $V_{\rm env}$ and transmissivity η. The symplectic spectral density $\overline{\nu}_\xi$ goes always up by increasing N (with respect to $\nu_\xi(N = 0)$), while ν_ξ goes always down (or does not change). Probably, for environment models showing correlation (memory) among modes, the presence of the second stage gives rise to capillary effects on the edges of the vessel resulting to a "water level" with meniscus form.

In Fig.4.4-left the classical capacity for Ω-model is plotted versus s for different values of η and fixed N, $N_{\rm env}$. The limit of the one shot capacity (3.24) when $s \to \infty$ is still valid. Presumably, as one can see from Fig.4.4-right, this limit is valid in the more general case of function[3] $\max_{V_{\rm env}}(\underline{C})$ when $M_{\rm env} \to \infty$.

4.2 Exact solution

To find the exact solution for Ω-model, one needs to completely characterize analytically "threshold functions" (3.27) and (3.28) as depending on mode parameter ξ (after taking the limit $n \to \infty$). That would allow to find all possible stages distributions and write the equations for the bounds between stages.

however the approximated chain (3.44) is used.

[3]The maximum is taken over arbitrary admissable environments $V_{\rm env}$ which have the same $M_{\rm env}$.

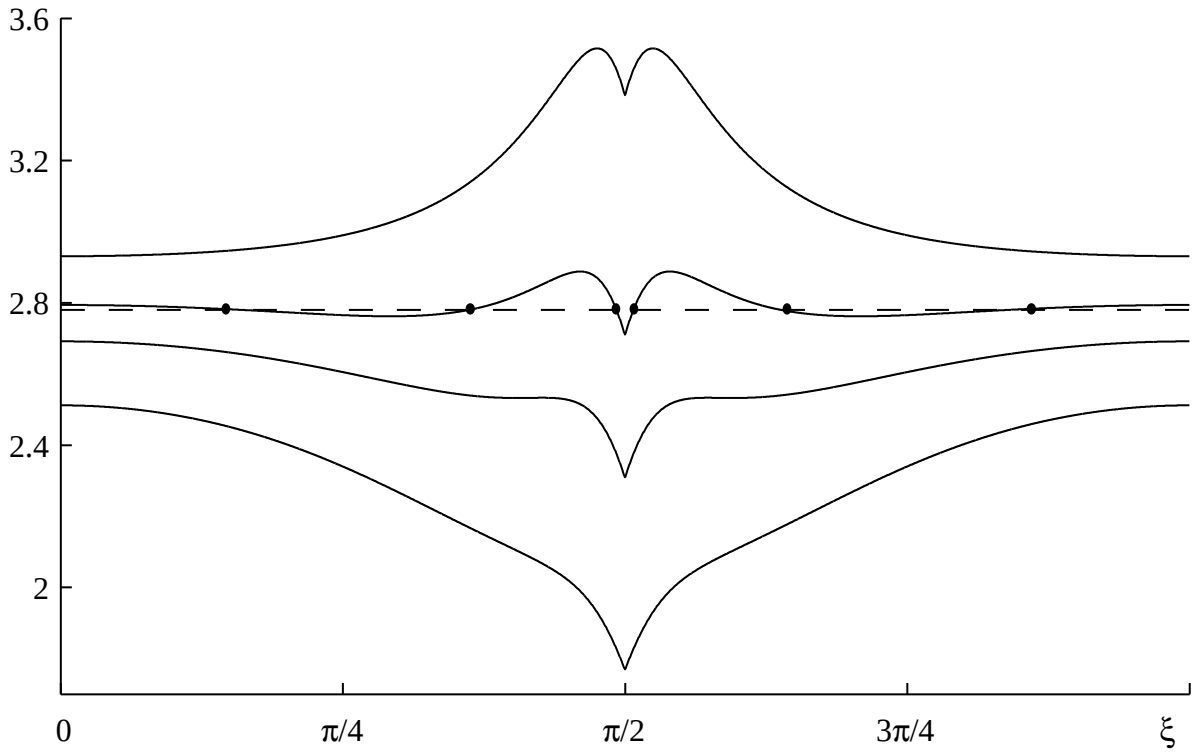

Figure 4.5: The quantity $\mathrm{thr}_{1\to 2}$ is plotted vs ξ for Ω-model for values of $\eta = 0.25, 0.32, 0.37, 0.45$ going from bottom to top curve. The value of other parameters are $N_{\mathrm{env}} = 0.01$, $s = 1$. The horizontal line corresponds to some value of energy constraint N (or, equivalently, λ) and crosses function $\mathrm{thr}_{1\to 2}(\xi)$ in the points of stages' transitions. The curve corresponding to the value of $\eta = 0.32$ has (approximately) its saddle-point where two of three roots of equation $\mathrm{thr}_{1\to 2}(\xi) = const.$ coincide.

Let us introduce the notations:

$$O_{qx} = \frac{\eta}{2} + (1-\eta)\left(N_{\mathrm{env}} + \frac{1}{2}\right)x, \qquad O'_{px} = -(1-\eta)\left(N_{\mathrm{env}} + \frac{1}{2}\right)\frac{1}{x^2},$$

$$O_{px} = \frac{\eta}{2} + (1-\eta)\left(N_{\mathrm{env}} + \frac{1}{2}\right)\frac{1}{x}, \qquad O''_{px} = 2(1-\eta)\left(N_{\mathrm{env}} + \frac{1}{2}\right)\frac{1}{x^3},$$

$$\mu'_x = \frac{\eta(1-\eta)}{2}\left(N_{\mathrm{env}} + \frac{1}{2}\right)\left(1 - \frac{1}{x^2}\right), \qquad \mu''_x = \eta(1-\eta)\left(N_{\mathrm{env}} + \frac{1}{2}\right)\frac{1}{x^3},$$

$$\mu_x = \frac{\eta^2}{4} + (1-\eta)^2\left(N_{\mathrm{env}} + \frac{1}{2}\right)^2 + \frac{\eta(1-\eta)}{2}\left(N_{\mathrm{env}} + \frac{1}{2}\right)\left(x + \frac{1}{x}\right),$$

where $x := e^{2s\cos\xi}$ (this eliminates the variable s from the equations) and $\mu_x \equiv \nu_x^2$. Then,

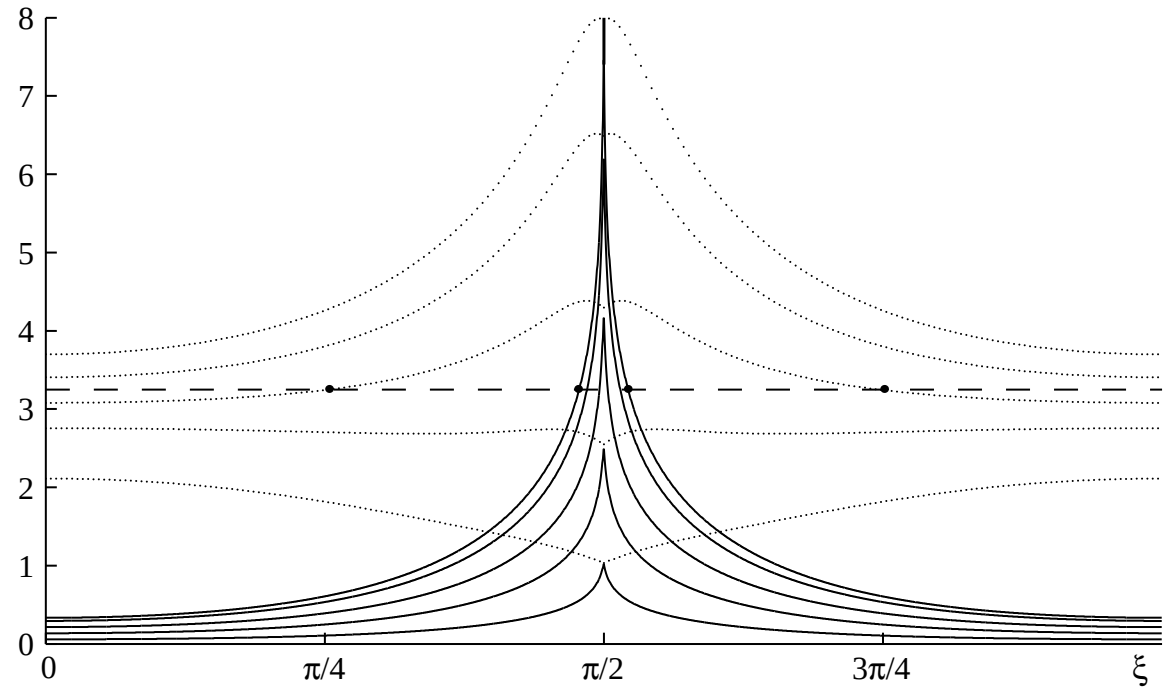

Figure 4.6: The quantities $\mathrm{thr}_{1\to 2}$ and $\mathrm{thr}_{2\to 3}$ are plotted vs ξ for Ω-model for values of $\eta = 0.15, 0.35, 0.55, 0.75, 0.85$ going from bottom to top curve. The value of other parameters are $N_{\mathrm{env}} = 0.01$, $s = 1$. The horizontal line corresponds to some value of energy constraint N (or, equivalently, λ) and crosses these threshold functions in the points of stages' transitions.

the threshold (3.27) with its derivatives can be written as

$$\mathrm{thr}_{1\to 2}(x) = \frac{\eta}{O_{px}} g_1, \tag{4.9}$$

$$\mathrm{thr}'_{1\to 2}(x) = \frac{\eta}{O_{px}} \left[\frac{g_1 + g_2}{2\mu_x} \mu'_x - \frac{O'_{px}}{O_{px}} g_1 \right],$$

$$\mathrm{thr}''_{1\to 2}(x) = \frac{\eta}{O_{px}} \left[\frac{g_2 - g_1 + g_3}{4\mu_x^2} \mu'^2_x + \frac{g_1 + g_2}{2\mu_x} \left(\mu''_x - \frac{O'_{px}}{O_{px}} (\mu'_x + 1) \right) - g_1 \left(\frac{O''_{px}}{O_{px}} - \frac{2O'^2_{px}}{O^2_{px}} \right) \right],$$

where all g_k-functions have the argument $\sqrt{\mu_x}$. In particular, saddle-point (see Fig.4.5) corresponds to x which is a root of the system of equations

$$\begin{cases} \mathrm{thr}'_{1\to 2}(x) = 0, \\ \mathrm{thr}''_{1\to 2}(x) = 0. \end{cases}$$

The quantities $\mathrm{thr}_{1\to 2}(\xi)$ and $\mathrm{thr}_{2\to 3}(\xi)$ (see Eqs. (4.9) and (3.28)) are plotted in Fig.4.6 as functions of ξ for different values of η and fixed s, N_{env}.

In explicit form the threshold $\mathrm{thr}_{1\to 2}$ can be written as

$$\mathrm{thr}_{1\to 2}(\xi) = \eta \sqrt{\frac{\frac{\eta}{2} + (1-\eta)(N_{\mathrm{env}} + \frac{1}{2}) e^{2s\cos\xi}}{\frac{\eta}{2} + (1-\eta)(N_{\mathrm{env}} + \frac{1}{2}) e^{-2s\cos\xi}}} g' \left(\nu_\xi(N=0) - \frac{1}{2} \right)$$

and should be analyzed as the function of $\xi \in (0, \pi/2)$ depending on parameters s, η and $N_{\rm env}$. Despite the threshold $\mathrm{thr}_{2\to3}$ given by Eq. (3.28) has simple form and monotonic over ξ for all parameters s, η and $N_{\rm env}$, the threshold $\mathrm{thr}_{1\to2}$ is not simple. E.g. the equation $\mathrm{thr}_{1\to2}(\xi) = const$ can have three different roots, which does not allow to write simple stages distribution similar to that in approximate solution discussed in previous section. This problem is currently under investigation.

4.3 Environment purity theorem

The following theorem related with purity of channel environment can be proved.

> Theorem: The maximum of capacity over the set of environment states $\{V_{\rm env}\}$ with fixed average amount of photons $M_{\rm env}$ can be achieved on pure state $V_{\rm env}$, *i.e.*
> $$e_{uk} e_{u_\star k} = 1/4.$$

Proof: At first, notice that the following Lemma takes place.

> Lemma: Suppose, that real numbers $a, b, c, d > 0$, $d > b$, $a - b > c - d$ and $f(x)$ is monotonically growing concave function in interval $x \in (0, \infty)$, then
> $$f(a) - f(b) > f(c) - f(d).$$

The environment model for multi-mode channel can be represented as

$$V_{\rm env} = \bigoplus_{k=1}^{n} V_{\rm env}^{(k)}, \quad \text{where} \quad V_{\rm env}^{(k)} = \left(N_{\rm env}^{(k)} + \frac{1}{2} \right) \begin{bmatrix} e^{s_k} & 0 \\ 0 & e^{-s_k} \end{bmatrix},$$

$$M_{\rm env} = \frac{1}{n} \sum_{k=1}^{n} M_{\rm env}^{(k)}, \quad \text{where} \quad M_{\rm env}^{(k)} = \left(N_{\rm env}^{(k)} + \frac{1}{2} \right) \cosh(s_k) - \frac{1}{2}.$$

If the kth mode belongs to the first stage, then $C_k \equiv 0$. If the kth mode belongs to the third state, then (see Eq. (3.40))

$$\max_{N_{\rm env}^{(k)}} C_k = C_k(N_{\rm env}^{(k)} = 0),$$

i.e. it is optimal to make the kth mode pure. Remember, that is was proved for $e_{qk} > e_{pk}$ and $c_{qk} = 0$ that $o_{qk} > a_{pk} > o_{pk}$ (see Eq. (3.5)).

Let us now change variables for kth mode by preserving $M_{\rm env}^{(k)}$ and making new $N_{\rm env}^{\prime(k)} = 0$ (the eigenvalues i_{uk} and c_{uk} remain the same): $e_{qk} \to e'_{qk}$, $e_{pk} \to e'_{pk}$. This results to $o'_{qk} > o_{qk}$ and $o'_{pk} < o_{pk}$, *i.e.* $o'_{qk} - o'_{pk} > o_{qk} - o_{pk}$, while $o'_{qk} + o'_{pk} = o_{qk} + o_{pk}$. It means that $\nu'_k < \nu_k$ (see analogous proofs in Subsec. 3.1.1).

One can then write down:

$$o'_{qk}(o'_{pk} + \eta c_{pk}) - o'_{qk} o'_{pk} > o_{qk}(o_{pk} + \eta c_{pk}) - o_{qk} o_{pk},$$

which is equivalent to $o'_{qk} > o_{qk}$. Taking into account the above inequality and applying the Lemma for $f(x) = \sqrt{x}$ one gets

$$\sqrt{o'_{qk}(o'_{pk} + \eta c_{pk})} - \sqrt{o'_{qk} o'_{pk}} > \sqrt{o_{qk}(o_{pk} + \eta c_{pk})} - \sqrt{o_{qk} o_{pk}}\,,$$

i.e. $\overline{\nu}'_k - \nu'_k > \overline{\nu}_k - \nu_k$. Finally, applying again the Lemma for the function $f(x) = g_0(x - 1/2)$ one gets $C'_k > C_k$. ■

Thus, optimal environment $V_{\rm env}$ can be always chosen in pure state, where each kth mode is completely characterized by its squeezing s_k. The important and still open question is the form of function $s(k)$ (or $s(\xi)$ for the case of $n \to \infty$) which gives the optimal channel memory. As it will be shown in the next section, this function is not a constant.

4.4 Violation of quadrature and mode symmetries: role of memory

Finally, let us discuss the role of squeezing and memory in lossy bosonic channel. Considering the lower bound (3.14) as a function on the set of environment models with fixed $M_{\rm env}$, one can see that it shows a *symmetry breaking over quadratures*. In fact despite the symmetry of all equations over quadratures, the maximum of $\underline{C}$ is achieved when $e_q \neq e_p$. This also follows from the above environment purity theorem applied to the single-mode channel.

Now let us analyze the symmetry of the capacity over modes. Suppose, that the average amount of photons in the environment $M_{\rm env}$ is fixed and the capacity $\underline{C}$ for memoryless and memory channel (for Ω-model) is compared. As far as the Holevo-χ quantity (1.28) is symmetric over modes one can expect that the capacity for memoryless channel will always be higher. However, this is not true as results from the *symmetry breaking over modes*. Actually, this can be seen in Fig.4.4-right where the capacity $\underline{C}$ maximized over parameters s, $N_{\rm env}$ (thus, always $N_{\rm env} = 0$) for memory and for memoryless cases is plotted versus $M_{\rm env}$.

Conclusions and outlook

In conclusion, a powerful and versatile tool for the estimation of Gaussian quantum channels capacities and transmission rates was developed in this thesis. It is based on the perturbative expansion of the von Neumann entropy of Gaussian states as function of the symplectic eigenvalues of the quadratures covariance matrix [9]. This method was applied to lossy bosonic channels. The found lower bounds on classical capacity are reliable rates of communication which can be achieved using solely Gaussian states for encoding classical information. Thus, this thesis generalizes the results of Refs. [31], [11] and [4]. The expansion of the von Neumann entropy can be as well applied for the evaluation and optimization of other entropic functions.

One can define a wide set of Gaussian channels which have the same capacity. Their environment covariance matrices are related each other by rotations which are simultaneously orthogonal and symplectic. The simplest channels from this set are those with diagonal matrices, thus their symplectic eigenvalues and energy restrictions are functions on the same matrix spectra. In turn, the approach proposed in this thesis can be extended to other capacities and Gaussian channels when the problem is spectral (the analysis for the additive noisy channel is currently ongoing at QuIC group of Universitè Libre de Bruxelles). Thus, the problems related with finding quantum, private and classical-assisted capacities (whose properties are still not well known) can be considered as the next ones for investigation, as tools already developed in this thesis should help essentially with their solution.

Let us discuss in detail the results obtained. A method to *analytically* calculate classical capacities and transmission rates of Gaussian quantum channels is found when the corresponding optimization problem is spectral. Algorithms suggested for the solution of this problem use some recent achievments in optimization theory where the problem is known as "convex separable minimization" [32]. Two algorithms (*static* and *dynamic*) were proposed in this thesis to solve the problem. The static algorithm is equivalent to the approach suggested in [32], while dynamic algorithm is essentially faster for this task, and it is simpler to proof.

Beside classical capacity, *analytical* relations expressing heterodyne and homodyne rates through quantum states covariance matrices were found for lossy bosonic channel with memory. It was shown that these rates do not reach the capacity except of some limit cases. It was found that both heterodyne and homodyne rates are closely related with a zeroth-order approximation to classical capacity. In particular, the homodyne rate coincides with this approximation for low energy restriction at channel input, while the heterodyne rate equals this approximation calculated for modified channel environment. Furthermore, all quantities related with the heterodyne rate get a simple form after suitably re-expressing

the involved eigenvalues and matrices.

The classical capacity was shown to depend only on the input energy constraint N and on the average amount of environment photons $M_{\rm env}$, when N is above a threshold value. In this case the type of memory does not play any role if environment is pure, and can affect capacity only through modes' $M_{\rm env}$s. By considering the behavior of the classical capacity as function of $M_{\rm env}$, the existence of *critical channel parameters* was discovered. It was found that lossy bosonic channel has two of these parameters: *critical beam-splitter transmissivity* $\eta^\star$ and *critical thermal environment photons* $N^\star_{\rm env}$ which are related according to the equation $(1-\eta^\star)(N^\star_{\rm env}+1/2) = 1/\sqrt{12}$. In particular, the value of critical transmissivity for pure channel environment is equal to $1-1/\sqrt{3}$. The parameter $N^\star_{\rm env}$ also exists for additive noise channel.

These critical parameters reveal themselves as follows. Suppose, that the capacity is analyzed as function of $M_{\rm env}$ for fixed $N_{\rm env}$ (it corresponds to variation of environment squeezing s) or η (if η is fixed, then functions corresponding to different parameters of $N_{\rm env}$ are considered, and vice versa). For such functions the optimal squeezing $s^\star$ (or, equivalently, optimal $M^\star_{\rm env}$) is finite if transmissivity $\eta > \eta^\star$ (or, for the other set of functions, $N_{\rm env} < N^\star_{\rm env}$) and infinite otherwise (the parameter N is always fixed in this consideration). These critical parameters probably do not depend on any other channel parameters including the type of memory model which make them fundamental quantities associated with the classical capacity of any Gaussian channel.

The study of the dependence of capacity from $M_{\rm env}$ also revealed *violation of quadrature* and *mode symmetry* in lossy bosonic memory channel. It means that either memory or memoryless channels may be preferable (depending on the channels parameters) to achieve higher capacity. This also poses the question on the type of *optimal memory model* which is characterized by pure environment. Consequently entanglement becomes useful for information transmission when higher squeezing is optimal, as far as entanglement is related to multimode squeezing. It was also shown that if environment state is squeezed, optimal input state is usually squeezed too. Such the properties can have the same nature as a *quantum phase transition* found in [36] for *qubit memory channels*.

The above results were demonstrated on a particular model to describe memory effects in a lossy bosonic channel. Memory effects in this model have nontrivial long range correlations (non-Markovian). Notwithstanding, the model has allowed to characterize the channel over an arbitrary number of uses for classical information transmission. As such it represents one of the seminal works studying the asymptotic behavior of a Gaussian memory channel.

Appendix

A. Eigenvalues for Ω-model

Let us consider the $n \times n$ matrix

$$\Omega = \begin{pmatrix} 0 & 1 & 0 & \dots & \dots & 0 \\ 1 & 0 & 1 & 0 & \dots & 0 \\ 0 & 1 & 0 & 1 & 0 & \dots & 0 \\ \vdots & \ddots & \ddots & \ddots & \ddots & \ddots & \vdots \\ 0 & \dots & 0 & 1 & 0 & 1 & 0 \\ 0 & \dots & \dots & 0 & 1 & 0 & 1 \\ 0 & \dots & \dots & 0 & 1 & 0 \end{pmatrix}.$$

Its eigenvalues are values λ such that the equation

$$\Omega x = \lambda x \tag{4.10}$$

has non-zero solution with respect to vector x. One way to obtain the eigenvalues of Ω is to note that $\Omega = 2I - T$, where I is identity matrix and T is the following $n \times n$ matrix:

$$T := \begin{pmatrix} 2 & -1 & 0 & \dots & \dots & 0 \\ -1 & 2 & -1 & 0 & \dots & 0 \\ 0 & -1 & 2 & -1 & 0 & \dots & 0 \\ \vdots & \ddots & \ddots & \ddots & \ddots & \ddots & \vdots \\ 0 & \dots & 0 & -1 & 2 & -1 & 0 \\ 0 & \dots & \dots & 0 & -1 & 2 & -1 \\ 0 & \dots & \dots & 0 & -1 & 2 \end{pmatrix}.$$

Being a finite-difference counterpart of operator $-\frac{d^2}{dx^2}$, the matrix T is very important in computational mathematics and its properties are well studied. It can be shown by straightforward substitution that matrix T has the following eigenvalues [37]:

$$\lambda_j^{(T)} = 2\left(1 - \cos\frac{\pi j}{n+1}\right)$$

and j-th normalized eigenvector x_j has the components

$$v_{j,k}^{(T)} = \sqrt{\frac{2}{n+1}} \sin\frac{jk\pi}{n+1}, \quad k = 1, \dots, n.$$

Thus, the matrix Ω will have the same eigenvectors $v_j^{(T)}$ and its eigenvalues turn out to be

$$\lambda_j^{(\Omega)} = 2 - \lambda_j^{(T)} = 2\cos\frac{\pi j}{n+1}. \tag{4.11}$$

For any matrix such as

$$A = \frac{1}{2}\begin{pmatrix} e^{\gamma\Omega} & 0 \\ 0 & e^{-\gamma\Omega} \end{pmatrix}, \quad \gamma \in \mathbb{R}, \tag{4.12}$$

we get the eigenvalues

$$\lambda_{\pm,k}^{(A)} = \frac{1}{2}e^{\pm 2\gamma\cos\left(\frac{\pi k}{n+1}\right)}, \tag{4.13}$$

as direct consequence of Eq.(4.11).

Another, more constructive way to derive eigenvalues of Ω is to treat the system of linear equations (4.10) as recurrence equation

$$x^{(k-1)} + \lambda x^{(k)} + x^{(k+1)} = 0, \quad k = 1, \ldots, n \tag{4.14}$$

with boundary conditions

$$x^{(0)} = 0, \quad x^{(n+1)} = 0. \tag{4.15}$$

In order to solve it, we first write characteristic equation

$$q^2 + \lambda q + 1 = 0. \tag{4.16}$$

Then, if the roots of characteristic equation q_1 and q_2 are different (non-degenerate case), general solution of Eq. (4.14) has the form [38]:

$$x^{(k)} = C_1 q_1^k + C_2 q_2^k,$$

where C_1 and C_2 are chosen to satisfy boundary conditions (4.15). If the roots are equal ($q_1 = q_2 = q$) we have degenerate case and the general solution is

$$x^{(k)} = C_1 q^k + C_2 k q^k.$$

It can be seen from Eq. (4.16) that in degenerate case $\lambda = \pm 2$.

Let us impose boundary conditions (4.15). In degenerate case $q = \pm 1$, therefore (4.15) yields $C_1 = 0$ and $C_2 = 0$. Since we are interested in non-zero solutions of (4.10) degenerate case gives no eigenvalues and we conclude that $\lambda \neq \pm 2$.

In non-degenerate case $C_2 = -C_1$ and $C_1\left(q_1^{n+1} - q_2^{n+1}\right) = 0$. Since solution is non-trivial one,

$$\left(\frac{q_1}{q_2}\right)^{n+1} = 1. \tag{4.17}$$

From (4.16) we obtain $q_{1,2} = -\frac{\lambda}{2} \pm \sqrt{\left(\frac{\lambda}{2}\right)^2 - 1}$. After substituting $q_{1,2}$ into (4.17) we arrive at the equation

$$\left(\frac{\frac{\lambda}{2} - \sqrt{\left(\frac{\lambda}{2}\right)^2 - 1}}{\frac{\lambda}{2} + \sqrt{\left(\frac{\lambda}{2}\right)^2 - 1}}\right)^{n+1} = 1$$

and finally we obtain the equation for eigenvalues of matrix Ω:

$$\frac{\frac{\lambda}{2}-\sqrt{\left(\frac{\lambda}{2}\right)^2-1}}{\frac{\lambda}{2}+\sqrt{\left(\frac{\lambda}{2}\right)^2-1}}=e^{i\frac{2\pi k}{n+1}},\quad k=1,\ldots,n. \tag{4.18}$$

$k\neq 0$ since it corresponds to degenerate case. Let us represent $\lambda/2$ as $\cosh\chi$, then previous relation can be rewritten as

$$\tanh\chi=\frac{1-e^{i\frac{2\pi k}{n+1}}}{1+e^{i\frac{2\pi k}{n+1}}}$$

or

$$\tanh\chi=\tanh\left(\frac{i\pi k}{n+1}\right)$$

and

$$\chi=\frac{i\pi k}{n+1}+2\pi i m,$$

where m is any whole number. Consequantly, we get eigenvalues of Ω-matrix (4.11).

Interesting to note that $(\Omega-\lambda I)$-matrix is a particlulary case of $n\times n$ 3-diagonal matrix known in linear algebra:

$$\Omega_{\text{general}}=\begin{pmatrix}\alpha+\beta & \alpha\beta & \ldots\ldots\ldots\ldots & & 0\\ 1 & \alpha+\beta & \alpha\beta & \ldots\ldots & 0\\ \vdots & 1 & \alpha+\beta & \alpha\beta \quad \ldots & 0\\ \vdots & \vdots & \ddots & \ddots \quad \ddots & \\ \vdots & \vdots & & \ddots \quad \ddots & \alpha\beta\\ 0 & 0 & \ldots\ldots\ldots & 1 & \alpha+\beta\end{pmatrix}.$$

Its has the determinant [39]:

$$\det\Omega_{\text{general}}=\frac{\alpha^{n+1}-\beta^{n+1}}{\alpha-\beta}. \tag{4.19}$$

If we put

$$\begin{aligned}\alpha&=-\tfrac{\lambda}{2}+\sqrt{\left(\tfrac{\lambda}{2}\right)^2-1},\\ \beta&=-\tfrac{\lambda}{2}-\sqrt{\left(\tfrac{\lambda}{2}\right)^2-1}\end{aligned} \tag{4.20}$$

we obtain characteristic equation for Ω-matrix (4.18).

B. Trace properties for Ω-model

We show that dealing with matrices of the form of Eq.(4.12), the average number of photons per mode remains finite even in the limit $n\to\infty$. To this end we consider

$$\lim_{n\to\infty}\frac{\mathrm{Tr}(A)}{2n}=\lim_{n\to\infty}\frac{\mathrm{Tr}(A)}{2(n+1)}=\frac{1}{4}\left(\lim_{n\to\infty}\frac{\mathrm{Tr}(e^{\gamma\Omega})}{n+1}+\lim_{n\to\infty}\frac{\mathrm{Tr}(e^{-\gamma\Omega})}{n+1}\right). \tag{4.21}$$

By taking into account Eq.(4.13) we can rewrite the first term at right-hand side of Eq.(4.21) as

$$\lim_{n\to\infty}\frac{\mathrm{Tr}(e^{\gamma\Omega})}{n+1}=\lim_{n\to\infty}\frac{\sum_{k=1}^{n}e^{2\gamma\cos\frac{\pi k}{n+1}}}{n+1}.$$

This relation is the limit of Riemann sum becoming an integral for the function $f(x)=e^{2\gamma\cos\pi x}$. This leads to a modified Bessel function of the first kind and zero-order [40]

$$\lim_{n\to\infty}\frac{\mathrm{Tr}(e^{\gamma\Omega})}{n+1}=\int_0^1 e^{2\gamma\cos\pi x}\,dx=\frac{1}{\pi}\int_0^{\pi}e^{2\gamma\cos\xi}\,d\xi=I_0(2\gamma).$$

Since the Bessel finction I_0 is even, the result of Eq.(4.21) is $I_0(2\gamma)/2$ whose asymptotic behavior is $e^{2\gamma}/(4\sqrt{\pi\gamma})$ for large γ. The existence of a finite limit in Eq.(4.21) allows us to conclude that the considered matrices (similar to Eq. (4.12)) give rise to a physical model.

C. Properties of g-function

Von Neumann entropy of Gaussian state involves consideration of g-function [8]:

$$g\left(v-\frac{1}{2}\right):=\left(v+\frac{1}{2}\right)\log_2\left(v+\frac{1}{2}\right)-\left(v-\frac{1}{2}\right)\log_2\left(v-\frac{1}{2}\right),\tag{4.22}$$

where v is a symplectic eigenvalue of the covariance matrix characterizing a Gaussian state. Despite the absence of a small parameter for the expansion of the function g, we proceed as follows. The function $g(v-1/2)$ is not analytic in neighbourhood of $1/2$ and infinity, however after subtracting the logarithm part it becomes analytic on the region $v\geqslant 1/2$. Hence, we may write (see also [9])

$$g\left(v-\frac{1}{2}\right)=\log_2 v+\frac{1}{\ln 2}\left[1-\frac{1}{2}\sum_{j=1}^{\infty}\frac{(2v)^{-2j}}{j(2j+1)}\right].\tag{4.23}$$

Thus, to the zeroth-order approximation we have

$$g\left(v-\frac{1}{2}\right)\approx\log_2 v+\frac{1}{\ln 2},\tag{4.24}$$

where we have neglected terms of the order $O(1/v^2)$, and in the first-order approximation it is

$$g\left(v-\frac{1}{2}\right)\approx\log_2 v-\frac{1}{(24\ln 2)v^2}+\frac{1}{\ln 2}.\tag{4.25}$$

Allowing perturbation of logarithm by the first terms in the series (4.23) we can also construct next-order approximations.

It is convenient to use function

$$g_k(v)=v^k g^{(k)}(v-1/2).\tag{4.26}$$

Thus, $g_0(v)=g(v-1/2)$, $g_1(v)=vg'(v-1/2)$ and so on. It also has simple rules to take derivatives, e.g.:

$$g_1'(v)=\frac{g_1(v)+g_2(v)}{v},\qquad g_2'(v)=\frac{2g_2(v)+g_3(v)}{v},\qquad g_1''(v)=\frac{2g_2(v)+g_3(v)}{v^2}.\tag{4.27}$$

In zeroth-order approximation $g_1(v)\equiv 1$.

Acknowledgments

I thank V. I. Man'ko who provided me with the basics of modern methods and approaches in quantum mechanics, without which this thesis work would not have been done. I also thank my adviser S. Mancini and my collaborator C. Lupo for their great help with basics of quantum information theory, which allowed me to concentrate more on formal mathematical problems related to quantum channels.

I thank V. G. Zborovskii for his great help with the most difficult mathematical problems arisen in this thesis, which finally allowed me to give a formal proof for the algorithm suggested to estimate rates and classical capacity. I also thank E. Karpov for his careful reading of my paper manuscript and further fruitful discussions on the topic, which helped to reveal some errors in first manuscript version of [A5] published in arXiv.

I thank Yu. N. Maltsev who gave me his lectures on linear algebra in Altai State University which helped me later a lot with the study of quantum mechanics. He also showed me a way to find analytically eigenvalues for a correlation matrix.

Bibliography

[1] Holevo A. S., "On the mathematical theory of quantum communication channels", *Probl. Inf. Transm.* vol. 8, pp. 62–71, 1972.

[2] Bennett C. H., and Shor P. W., "Quantum information theory", *IEEE Trans. Inf. Th.* vol. 44, pp. 2724–2742, 1998.

[3] Kretschmann D., and Werner R. F., "Quantum channels with memory", *Phys. Rev. A* vol. 72, pp. 062323-1–052324-19, 2005.

[4] Giovannetti V., and Mancini S., "Bosonic Memory Channels", *Phys. Rev. A* vol. 71, pp. 062304-1–062304-6, 2005.

[5] Cerf N., Clavareau J., Macchiavello C., and Roland J., "Quantum entanglement enhances the capacity of bosonic channels with memory", *Phys. Rev. A* vol. 72, p. 042330, 2005; Cerf N., Clavareau J., Roland J., and Macchiavello C., "Information transmission via entangled quantum states in Gaussian channels with memory", *Int. J. of Quant. Inf.* vol. 4, pp. 439–452, 2006.

[6] Ruggeri G., and Mancini S.," Quantum Gaussian channels with additive correlated classical noise", *Quant. Inf. & Comp.* vol. 7, pp. 265–272, 2007.

[7] Ruggeri G., and Mancini S., "Privacy of a lossy bosonic memory channel", *Phys. Lett. A* vol. 362, pp. 340–343, 2007.

[8] Holevo A. S., and Werner R. F., "Evaluating capacities of Bosonic Gaussian channels", *Phys. Rev. A* vol. 63, pp. 032312-1–032312-14, 2001.

[9] Holevo A. S., Sohma M., and Hirota O., "Capacity of quantum Gaussian channels", *Phys. Rev. A* vol. 59, pp. 1820–1828, 1999.

[10] Braunstein S. L., and Pati A. K., *Quantum Information Theory with Continuous Variables*, Dordrecht, Kluwer Academic, 2003; Braunstein S. L. and van Loock P. *Rev. Mod. Phys.* vol. 77, p. 513, 2005.

[11] Giovannetti V., Guha S., Lloyd S., Maccone L., Shapiro J. H., and Yuen H. P., "Classical capacity of the lossy bosonic channel: the exact solution", *Phys. Rev. Lett.* vol. 92, pp. 027902-1–027902-4, 2004.

[12] Giovannetti V., Lloyd S., Maccone L., and Shor P. W., "Entanglement assisted capacity of the broadband lossy channel", *Phys. Rev. Lett.* vol. 91, pp. 047901-1–047901-4, 2003.

[13] Wolf M. M., Perez-Garcia D., and Giedke G., "Quantum Capacities of Bosonic Channels", *Phys. Rev. Lett.* vol. 98, pp. 130501-1–130501-4, 2007.

[14] Cover T. M., and Thomas J. A., *Elements of Information Theory*, New York, Wiley-Interscience, 1991.

[15] R. L. Stratonovich, "On distributions in representation space", *Sov. Phys. JETP* vol. 4, pp. 891–898, 1957.

[16] H. Weyl, "The Theory of Groups and Quantum Mechanics", Dover, 1932.

[17] E. Wigner, "On the Quantum Correction For Thermodynamic Equilibrium", *Phys. Rev.* vol. 40, pp. 749–759, 1932.

[18] K. Husimi, "Some formal properties of the density matrix", *Proc. Phys. Math. Soc. Jpn.* vol. 23, pp. 264–314, 1940.

[19] K. E. Cahill, and R. J. Glauber, "Density Operators and Quasiprobability Distributions", *Phys. Rev.* vol. 177, pp. 1882–1902, 1969.

[20] M. A. Nielsen, and I. L. Chuang, "Quantum computation and quantum information", Cambridge University Press, 2000.

[21] D'Ariano G. M., "Quantum Estimation Theory and Optical Detection", in *Quantum Optics and Spectroscopy of Solids*, T. Hakioglu and A. S. Shumovsky Eds. Kluwer, p. 139, 1997.

[22] M. de Gosson, "Symplectic Geometry and Quantum Mechanics: Operator Theory, Advances and Applications" vol. 166, Birkhäuser, 2006.

[23] Holevo A. S., "Statistical problems in quantum physics", in: Maruyama G. and Prokhorov J. V. (eds.), Proceedings of the Second Japan-USSR Symposium on Probability Theory, pp. 104–119, Springer-Verlag, Berlin, 1973; Lecture Notes in Mathematics, vol. 330.

[24] Gordon J. P., "Noise at optical frequences: information theory", in: Miles P. A. (ed.), "Quantum electronics and coherent light", Proceedings of the International School of Physics 'Enrico Fermi' XXXI, Academic Press, New York, 1964.

[25] Holevo A. S., "Quantum coding theorems", *Russ. Math. Surveys* vol. 53, pp. 1295-1331, 1998.

[26] Schumacher B., and Westmoreland M. D., "Sending classical information via noisy quantum channels", *Phys. Rev. A* vol. 56, pp. 131-138, 1997.

[27] Schäfer J., Daems D., Karpov E., and Cerf N. J., "Capacity of a bosonic memory channel with Gauss-Markov noise", *Phys. Rev. A* vol. 80, pp. 062313-1–062313-11, 2009.

[28] Bertrand J., and Bertrand P., "A tomographic approach to Wigner's function", *Found. Phys.* vol. 17, pp. 397–405, 1987.

[29] Mancini S., Man'ko V. I., and Tombesi P., "Symplectic Tomography As Classical Approach To Quantum Systems", *Phys. Lett. A* vol. 213, pp. 1–6, 1996.

[30] Mancini S., Man'ko V. I., and Tombesi P., "Classical-Like Description Of Quantum Dynamics By Means Of Symplectic Tomography", *Found. Phys.* vol. 27, pp. 801–824, 1997.

[31] Caves C. M., Drummond P. D., "Quantum limits on bosonic communication rates", *Rev. Mod. Phys.* vol. 66, pp. 481–537, 1994.

[32] Stefanov S. M., "Convex Separable Minimization Subject to Bounded Variables", *Comp. Opt. Appl.* Vol. 18, pp. 27–48, 2001.

[33] Stefanov S. M., "Separable Programming. Theory and Methods", Kluwer Academic Publishers: Dordrecht- Boston-London, 2001.

[34] Lo C. F., and Sollie R., "Generalized multimode squeezed states", *Phys. Rev. A* vol. 47, p. 733–735, 1993.

[35] Datta N., and Dorlas T., "The coding theorem for a class of quantum channels with long-term memory", *J. Phys. A* vol. 40, pp. 8147–8164, 2007.

[36] Plenio M, and Virmani S., "Spin Chains and Channels with Memory", *Phys. Rev. Lett.* vol. 99, p. 120504-1–120504-4, 2007.

[37] Demmel J., *Applied numerical linear algebra,* SIAM, Philadelphia, PA, 1997.

[38] Samarskii A., *The theory of difference schemes.* Marcel Dekker, New York, 2001.

[39] Proskuryakov, *Sbornik zadatch po lineynoy algebre* [in russian], Moscow.

[40] Abramowitz M., and Stegun I. A., *Handbook of Mathematical Functions with Formulas, Graphs, and Mathematical Tables*, Dover, New York, 1964.